1-1-2009

Detrital zircon sedimentary provenance ages for the Eoarchaean Isua supracrustal belt southern West Greenland: Juxtaposition of an imbricated ca. 3700 Ma juvenile arc against an older complex with 3920-3760 Ma components

Allen P. Nutman
University of Wollongong, anutman@uow.edu.au

Clark R L Friend

Shane Paxton

Detrital zircon sedimentary provenance ages for the Eoarchaean Isua supracrustal belt southern West Greenland: Juxtaposition of an imbricated ca. 3700 Ma juvenile arc against an older complex with 3920-3760 Ma components

Abstract

The amphibolite facies Eoarchaean Isua supracrustal belt (northern part of the Nuuk region, southern West Greenland) is dominated by strongly deformed metabasalts, with chert, banded iron formation, felsic volcanic and volcano-sedimentary rocks and minor gabbro and sedimentary carbonates. It comprises a suture zone between a northern terrane formed at ca. 3700 Ma and a southern one formed at ca. 3800 Ma. At the junction between these two terranes is a strongly tectonised, thin unit of metachert, BIF and carbonate-bearing rocks with minor detrital components, named the dividing sedimentary unit. Away from the belt, the northern terrane is dominated by ca. 3700 Ma tonalites and the southern one by ca. 3800 Ma tonalites. The Isua supracrustal belt chemical metasedimentary rocks give low yields of small (commonly3750 Ma detrital zircons suggests that these volcanic assemblages evolved remote from 3800 Ma crust. In contrast, the up to 3940 Ma detrital zircons from the dividing sedimentary unit and the southern fuchsite quartzite shows that the southern ca. 3800 Ma terrane, although dominated by arc-related rocks, might contain older (pre-3800 Ma) crust. We propose that the dividing sedimentary unit was deposited on top of already deformed southern terrane rocks, and then acted as a decollement when the northern terrane ca. 3700 Ma arc complex collided with the southern terrane by ca. 3660 Ma (from previous age constraints). Thus the detrital zircon age data is compatible with proposals from other evidence for juxtaposition of ca. 3700 and 3800 Ma terranes in the Isua area. Some thin siliceous metasedimentary rocks along post-assembly mylonite zones in the Isua supracrustal belt yield some(requiring confirmation) is that they could be younger, post-collisional sedimentary rocks, which were incorporated as tectonic lenses along some of the post-terrane-assembly

Keywords

older, against, arc, juvenile, ma, components, 3700, 3760, ca, imbricated, juxtaposition, greenland, west, southern, belt, supracrustal, isua, eoarchaean, ages, provenance, sedimentary, zircon, detrital, 3920, complex, GeoQUEST

Disciplines

Life Sciences | Physical Sciences and Mathematics | Social and Behavioral Sciences

Publication Details

Nutman, A. P., Friend, C. R L. & Paxton, S. (2009). Detrital zircon sedimentary provenance ages for the Eoarchaean Isua supracrustal belt southern West Greenland: Juxtaposition of an imbricated ca. 3700 Ma juvenile arc against an older complex with 3920-3760 Ma components. Precambrian Research, 172 (3-4), 212-233.

Detrital zircon sedimentary provenance ages for the Eoarchaean Isua supracrustal belt southern West Greenland: Juxtaposition of an imbricated ca. 3700 Ma juvenile arc against an older complex with 3940-3800 Ma components

Allen P. Nutman[a,b] Clark R.L. Friend[a] and Shane Paxton[b]

[a]Beijing SHRIMP Centre and Chinese International Centre for Precambrian Research, Chinese Academy of Geological Sciences,
26, Baiwanzhuang Road, Beijing, 100037 China
[b]Research School of Earth Sciences, The Australian National University, Canberra, ACT 0200, Australia
emails: nutman@bjshrimp.cn, crlfriend@yahoo.co.uk, Shane.Paxton@anu.edu.au

Abstract

The amphibolite facies Eoarchaean Isua supracrustal belt (northern part of the Nuuk region, southern West Greenland) is dominated by strongly deformed metabasalts, with chert, banded iron formation, felsic volcanic and volcanosedimentary rocks and minor gabbro and sedimentary carbonates. It comprises a suture zone between a northern terrane formed at ca. 3700 Ma and a southern one formed at ca. 3800 Ma. At the junction between these two terranes is a strongly-tectonised, thin unit of metachert, BIF and carbonate-bearing rocks with minor detrital components, named the *dividing sedimentary unit*. Away from the belt, the northern terrane is dominated by ca. 3700 Ma tonalites and the southern one by ca. 3800 Ma tonalites.

The Isua supracrustal belt chemical metasedimentary rocks give low yields of small (commonly ≤50 μm long), prismatic, oscillatory-zoned zircons with less common, somewhat rounded zircons of volcanic and/or detrital origin. The most siliceous of the felsic schists give a larger yield of volcanic or detrital zircons. The ages of these zircons are distinct in different parts of the belt. In the northern terrane, most have ages of 3710-3690 Ma, with a few slightly older <3750 Ma grains. In the southern 3800 Ma terrane, a fuchsite-quartzite has 3900-3810 Ma zircons. Three samples of the dividing sedimentary unit along the whole length of the belt yielded both 3940-3880 Ma (in two samples) and ca. 3750 Ma detrital zircons (in all three samples). The part of the ca. 3700 Ma northern terrane in the Isua supracrustal belt is interpreted as lithologically diverse and imbricated assemblage of ca. 3700 Ma arc-related volcanic rocks (boninitic, island arc tholeiite-picrite and andesite-dacite). In the associated metasedimentary rocks, the lack of >3750 Ma detrital zircons suggests that these volcanic assemblages evolved remote from 3800 Ma crust. In contrast, the up to 3940 Ma detrital zircons from the dividing sedimentary unit and the southern fuchsite quartzite shows that the southern ca. 3800 Ma terrane, although dominated by arc-related rocks, might contain older (pre-3800 Ma) crust. We propose that the dividing sedimentary unit was deposited on top of already deformed southern terrane rocks, and then acted as a décollement when the northern terrane ca. 3700 Ma arc complex collided with the southern terrane by ca. 3660 Ma (from previous age constraints). Thus the detrital zircon age data is compatible with proposals from other evidence for juxtaposition of ca. 3700 and 3800 Ma terranes in the Isua area.

Some thin siliceous metasedimentary rocks along post-assembly mylonite zones in the Isua supracrustal belt yield some <3660 Ma zircons. A tentative interpretation of these siliceous rocks (requiring confirmation) is that they could be younger, post collisional sedimentary rocks, which were incorporated as slivers along some of the post-terrane-assembly <3660 Ma mylonites which partition the collisional assemblage.

Keywords: Isua supracrustal belt, Eoarchaean, Greenland, terrane assembly, detrital zircon dating

1. Introduction

The Isua supracrustal belt (Fig. 1) in the northern part of the Itsaq Gneiss Complex (Nuuk district, southern West Greenland) is the world's largest known body of Eoarchaean metavolcanic and metasedimentary rocks (Nutman et al., 1996 and references therein). The antiquity of the rocks in the Isua area was demonstrated by whole rock Rb-Sr, Pb/Pb and then bulk zircon U-Pb and Sm-Nd whole rock isotopic dating methods (Moorbath et al., 1972, 1973; Hamilton et al., 1978; Michard-Vitac, 1977; Baadsgaard et al., 1984). One school of thought applied Sm-Nd whole rock dating to ascertain the age of the Isua rocks, and considered that there was essentially one package of supracrustal rocks, with an age of 3772±33 Ma (e.g. Moorbath and Whitehouse, 1996) or simply between 3800-3700 Ma (e.g., Myers, 2001). Another school of thought applied zircon geochronology to ascertain the age of the Isua rocks, and suggested that the belt contains unrelated volcanic rocks differing in age by about 100 million years (Nutman et al., 1996 page 17; Nutman et al. 1997, page 271). These data were interpreted to indicate that the belt contains several slices of supracrustal rocks of different origin and age that were tectonically juxtaposed in the Eoarchaean (e.g., Nutman et al., 1997, 2000, 2002, 2007a; Polat and Hofmann, 2003; Crowley, 2003). This latter view of different-aged packages has now become more widely accepted (e.g. Kamber et al. 2005).

For several reasons, obtaining the correct age for Isua supracrustal rocks is an important endeavour in understanding the early Earth. For example, their isotopic signatures are widely used to model or constrain early terrestrial planetary differentiation (e.g., Caro et al., 2003; Bennett et al., 2007), and metasedimentary rocks have been searched for evidence of early life (e.g. Mojzsis et al., 1996; Rosing et al., 1999). Furthermore, geochronology plays an important part in understanding the tectonic evolution of Isua, and thereby giving insight into early geodynamics. Most workers now view the tectonic evolution of Isua in a broadly plate tectonic framework, but their interpretations vary greatly. Thus Komiya et al. (1999) used the accretionary margin and ocean plate stratigraphy concepts developed in the Japanese archipelago to suggest that Isua contains the remnants of a single ancient accretionary complex. In this ocean plate stratigraphy model, all of the belt's cherts and other chemical sedimentary rocks should be tectonic repetitions of essentially the same sedimentary unit. Other workers have interpreted the Isua area to contain both ca. 3800 and ca. 3700 Ma juvenile crustal complexes, which were juxtaposed in the Eoarchaean, before ca. 3500 Ma Ameralik dykes were intruded (Nutman et al., 1997, 2002, 2007a; Crowley, 2003; Polat and Hoffman, 2003). In this latter interpretation, there is neither a requirement that different chert units exposed across the belt are coeval, nor that they should have the same detrital or volcanic zircon age spectra.

In this paper we approach this issue of the age of the Isua supracrustal rocks solely from the viewpoint of zircons extracted from chemical sedimentary rocks and felsic schists of volcanic or volcano-sedimentary in origin. Our results clearly support the models that Isua contains unrelated packages of rocks of different age, ca. 3800 Ma and ca. 3700 Ma (Figs 2 and 3).

2. Isua supracrustal belt U-Pb zircon geochronology

In Archaean gneiss complexes, 5 to 10 million year age resolution is necessary in order to distinguish rocks similar in appearance but of different age, and to resolve intra-terrane tectonothermal evolution. $^{207}Pb/^{206}Pb$ ages on zircons with concordant ages can achieve this resolution, with the correct choice of samples (e.g. Compston et al., 1986; Crowley, 2003). However, application of this method to the Isua supracrustal belt is not without problems. A major problem is that the belt is dominated by amphibolites derived from basaltic volcanic protoliths, such as pillow lavas (e.g. Komiya et al., 1999). Such volcanic protoliths rarely, if ever, carry igneous zircon, meaning that direct protolith ages cannot usually be obtained by this method. One approach to obtain minimum age constraints on mafic rocks is to date granitoid sheets that cut them (preferably juvenile tonalites). Tonalite sheets are quite common in the amphibolites along the southern side of the belt. These have yielded ages of ca. 3800 Ma, giving minimum eruption ages for the volcanic protoliths (Fig. 2d; Nutman et al., 1996, 1997, 2002; Crowley, 2003). However, such sheets are much rarer in the northern parts of the belt, but where found, they give ages of 3720-3710 Ma (Fig. 2a; Grimes and Dunning, 2002; Nutman and Friend, unpublished data), that were also interpreted as a minimum eruption age for the northern amphibolites.

There are also some units of felsic schists in the Isua supracrustal belt. Those at the eastern end (Fig. 1) are agreed by all workers to have been derived from volcanic and/or volcano-sedimentary rocks. All of these units have zircon ages of ca. 3700 Ma (Nutman et al., 1996, 1997; Kamber et al., 2005) that are best interpreted as the likely time for deposition of these rocks, thereby giving direct ages for some of the felsic volcanic activity in the belt.

The age of the youngest detrital zircons in sedimentary rocks can also be used as a useful age constraint for supracrustal sequences (e.g., Sircombe et al., 2001). However rocks of this type are very rare in the Isua supracrustal belt. Detrital zircon age provenance of a few Isua metasedimentary rocks presented by Nutman and Collerson (1991), Nutman et al. (1997, 2002, 2007a) and Kamber et al. (2005) showed

provenance contrasts between sedimentary units from different parts of the belt. Study of detrital zircon age provenance is extended here, with coverage of all the belt's major sedimentary rock units.

3. Isua metasedimentary rocks

3.1. Siliceous, iron-rich and carbonate rocks

Since the 1960s, cherts and magnetite-bearing banded iron formations (BIF) have been recognised and accepted as sedimentary components of the Isua supracrustal belt (Keto and Kurki, 1967; Moorbath et al., 1973; Dymek and Klien, 1988; Bohlar et al., 2004; Frei and Polat, 2005). These rocks have a discontinuous fine-scale layering of quartz + magnetite ± amphibole, which had been widely mistaken as simply strongly deformed sedimentary stratification, particularly in earlier studies (see e.g. Fig. 3A of Nutman et al., 1984). However, modern structural studies reveal this fine-scale layering to be entirely tectonic in origin, as witnessed by its development by both rotation of genuine sedimentary layering combined with growth of a new magnetite foliation around the margins of rare low strain lithons where sedimentary layering is preserved (see Fig. 5c, Nutman and Friend, this volume). Despite the high strain of most of these rocks, they retain seawater-like REE+Y trace element signatures, which reinforce their origin as chemical sediments (Fig. 4; Bohlar et al., 2004; Friend et al., 2007).

There is clear evidence in the Isua supracrustal belt of carbonate formation in veins during later tectonic activity which is clearly not related to depositional processes (e.g., Rosing et al., 1996; Polat and Hofmann, 2003). There are other carbonate-rich rocks associated with chert and BIF of uncontested chemical-sedimentary origin (Nutman et al., 1984; Dymek and Klein, 1988) that formed from mixtures of silica + Fe-dolomite ± siderite/hematite/magnetite (Nutman et al., 1984), and display seawater-like REE+Y patterns (Fig. 4; samples G04/54 and 55 of Friend et al., 2007). These chemical signatures show that these carbonate-bearing rocks either formed directly as sediments or are chert and BIF that were affected by low temperature (<100°C) diagenetic dolomitization. Regardless, this shows the protoliths of these particular carbonate-bearing rocks were sediments, rather than being higher-temperature metasomatic veins.

166

167 3.2. Zircons in Isua chemical metasediments

168 Chemical metasedimentary rocks from the belt have been shown to contain rare,
169 tiny, and generally prismatic zircons (Nutman et al., 2002). These zircons, with
170 euhedral to subhedral habit have fine-scale oscillatory zoning. If all the few zircons
171 from the different Isua chemical metasedimentary units showed the same age, and were
172 low Th/U and devoid of oscillatory zoning, an attractive origin for them would be by
173 growth *in situ* during Archaean metamorphism. However, this is not the case. These
174 zircons crystallised from 3940 to <3690 Ma with unique age signatures for each
175 geological unit (Fig. 2), oscillatory zoning is widely preserved, and they show high
176 Th/U (Table 1), typical of those grown from felsic magmas. Furthermore, laser
177 ablation ICPMS rare earth element (REE) analysis of zircons from two metacherts
178 G91/74 and IEh50ch display negative Eu anomalies in the chondrite normalised REE
179 patterns, apart from those where generally high light REE abundances (due to
180 hydrothermal processes?) swamped this signature (Fig. 5, Table 2 and analytical
181 method in Nutman and Friend, 2007). This suggests that they grew in the presence of
182 plagioclase. This is despite the plagioclase-free character of the host rocks. The
183 accumulated evidence leads us to interpret these rare zircons to be of felsic volcanic
184 and/or sedimentary origin, and provide provenance age information, rather than the age
185 of metamorphism. Thus they are interpreted to be related to low volume ash-fall or
186 fine-grained detrital pollutants into the chemical sedimentary rocks. Such zircons have
187 been observed in chemical sedimentary rocks elsewhere, such as in Palaeoproterozoic
188 rocks of South Africa and Western Australia (e.g., Pickard, 2003).

189

190 3.3. Felsic schists

191 There are two prominent units of felsic schists within the Isua supracrustal belt
192 (Allaart, 1976 onwards) and several thinner ones that are mostly intercalated with
193 amphibolites of boninitic chemical affinity (e.g. the Rosing 'early life' locality unit, for
194 which zircon data is presented below; Nutman et al., 1984; Rosing, 1999; Fedo et al.,
195 2001). Generally these units are very strongly deformed, such that original structures in
196 the protoliths have been destroyed. However, in the large felsic schist unit in the
197 northeast of the belt, there are low-strain domains where graded layering is preserved
198 (Fig. 3B of Nutman et al. 1984 and Fig. 2 of Nutman et al., 1997). Hence we interpret
199 these rocks as intermediate to felsic volcanic rocks, or sedimentary rocks derived by

rapid recycling of such source materials. Detailed trace element chemistry of these rocks (Bohlar et al., 2005) is in accord with this interpretation. More evolved (dacitic?) upper parts of this unit have yielded igneous zircons with ages of 3710-3700 Ma (Nutman et al., 1997; Kamber et al., 2005), which is interpreted to date the age of this volcanism.

Running the length of the Isua supracrustal belt is a unit of muscovite-bearing commonly carbonated felsic schists, which only yields ca. 3800 Ma igneous-like zircons that are prismatic with well developed oscillatory zoning (Michard-Vitrac et al., 1977; Baadsgaard et al., 1984; Compston et al., 1986; Nutman et al., 2002, 2007a; Hiess et al., in press). The abundance of zircons of this character indicates that the unit must consist of altered felsic igneous rocks, either volcanic (Allaart, 1976; Nutman et al., 1984) or a metasomatised tonalite sheet (e.g. Rosing et al., 1996). We will explore the origin of this unit in more detail elsewhere. However at this juncture it is worth noting that regardless of its volcanic or intrusive nature, its zircon ages show that the rocks spatially associated with it must be ≥3800 Ma, and thus ca. 100 million years older than felsic rocks in the northern side of the Isua supracrustal belt (Nutman et al., 1997).

4. Zircon geochronology

4.1. Analytical method

Previous Isua detrital zircon SHRIMP U-Pb age data were acquired on the SHRIMP-1, -2 and -RG instruments in the Australian National University (Nutman and Collerson, 1991; Nutman et al., 1996, 1997, 2002, 2007a). Data presented by Kamber et al. (2005) were obtained using the Cameca 1270 ion microprobe in Stockholm. These are integrated and reassessed with the new data presented here (Table 1). Where available, GPS positions (datum = WGS84) for samples are given, otherwise a less accurate position is given using the 1:40,000 map of Nutman (1986). Please note that these map coordinates and the WGS84 datum do not coincide.

Most of the new data were obtained using the SHRIMP-2 instrument (BJSHRIMP) at the Institute of Geology, Chinese Academy of Geological Sciences, with a lesser amount with the SHRIMP-RG instrument of the Australian National University. After crushing in a tungsten carbide mill, samples were gently “deslimed” (passing water through the sample in a large beaker to remove the finest fraction). This process was employed to try and retain any rare small zircons still suitable for

SHRIMP analysis (>15, <50 micron), yet remove the finest size fraction that would clog the ensuing mineral separation procedures. This was followed by separation of zircons using standard ANU heavy liquid and Franz isodynamic separator techniques. In cases where the samples contained a large amount of magnetite (particularly BIF), a preliminary stage was to put the sample under alcohol in a flat tray and then repeatedly pass over it a hand magnet wrapped in a plastic bag. This process removed most of the magnetite prior to isodynamic separation.

The separated zircons were mounted with FC1 reference zircons and cast in epoxy resin plugs. The cured plugs were very cautiously ground and polished to expose the zircon mid sections. Caution was needed, because the very small size of many of the zircons meant that they could be destroyed by polishing for even a couple of minutes too long. CL images were acquired of the zircons in order to select the least damaged domains for analysis. When permitting, a 20-25 μm spot was used for analysis, but for some samples the spot size was ca. 15 μm (with a proportionate increase of analytical errors because of less secondary ions to count).

$^{238}U/^{206}Pb$ in the unknowns was referenced to FC1 (considered concordant with an age of 1099 Ma; Paces and Miller, 1993). U was calibrated against fragments of the reference zircon crystal SL13 (238 ppm U) or 10095 (81.6 ppm U). Analytical protocols, calibration of data and calculation of analytical errors are summarised by Stern (1998) and Williams (1998).

4.2. Data appraisal

Each sample of metachert, BIF and carbonate of chemical sedimentary origin upon which zircon separations have been undertaken yielded between one and twenty eight zircons which with confidence can be considered to belong to the sample, rather than being laboratory contaminants. In previous reporting of the ages of tiny prismatic zircons from Isua metacherts (Nutman et al. 2002) and a BIF (Nutman et al., 2007a), it was assumed that all zircons were volcanic-derived (ash fall?) from a uniform-aged source. Likewise, the more abundant zircons separated from felsic schist units of volcanic or volcano-sedimentary origin, were interpreted to be uniform in age (Nutman et al., 1996, 1997). This approach was justified in samples where the ages of all grains were statistically indistinguishable from each other with a high level of confidence (i.e. Mean Squared Weighted Deviates (MSWD) ≤1). In other samples, however, such as

fuchsite-quartzite sample G93/25 reported by Nutman et al. (1997), the zircons clearly had distinguishable ages between ca. 3900 and 3810 Ma and hence were assessed as multi-component detrital populations. Data appraisal in this paper was facilitated by the Program ISOPLOT/EX (Ludwig, 2003) via cumulative frequency distribution diagrams combined with the data binned as histograms plus weighted mean $^{207}Pb/^{207}Pb$ age calculations.

In this paper we do *not* assume that any zircon analyses were part of an initially uniform single-aged population, in which any dispersion in apparent age is entirely due to minor loss of radiogenic Pb in ancient events(s). Instead, after rejecting or combining some data by the following procedures, the age of each zircon was considered of equal importance: First, any analyses of sites that are clearly heterogeneous or partly recrystallised in CL images[1] or via an optical microscopy examination were rejected. Second, sites whose $^{206}Pb/^{238}U$ versus $^{207}Pb/^{206}Pb$ ages differed by >10% or that have >2% of their ^{206}Pb derived from common sources based on measured ^{204}Pb (i.e. Pb not produced by *in situ* Uranium decay) were also rejected. This removed analyses with the most disturbed ages (Table 1).

For the remaining, less-disturbed zircon analyses, for which there was only a single analysis of the grain, this was assumed as an estimate of the grain's age, but strictly the minimum age. Where there were multiple analyses on a single grain, whose $^{207}Pb/^{206}Pb$ agreed within error (MSWD $\leq$1), a weighted mean $^{207}Pb/^{206}Pb$ age was calculated, which was taken as the age of the grain (Table 1). Where there were multiple analyses whose $^{207}Pb/^{206}Pb$ ages did not agree within error, it was assumed that some of the analysed sites had lost some radiogenic Pb in an ancient event, and these were not included in calculating a weighted mean $^{207}Pb/^{206}Pb$ age (with MSWD<1; e.g. grain 3, sample G05/28+29). In other cases, the dispersion in apparent ages was greater, such that none overlapped within error. In this situation, the oldest age was taken as an estimate of the age of the grain by using the loss of radiogenic Pb model (e.g. grain 7 of sample G93/28).

[1] Some zircon samples (see Table 1) were analysed in the early 1990s prior to use of CL imagery. This makes assessment of Pb loss in these samples more difficult.

296 *4.3. Northern ca. 3700 Ma terrane metacherts, BIF and carbonates*

297 4.3.1. Geological association. The northern ca. 3700 Ma terrane metacherts, BIF and
298 carbonates are generally strongly deformed, often to the extent of being mylonitic and
299 thoroughly recrystallised. Nonetheless, they form persistent structural markers. Also,
300 locally there are lenses of lower strain where sedimentary layering (albeit still
301 deformed) is still recognisable (e.g. Frei and Polat, 2005). These rocks are mostly
302 found bordering, and as intercalations within, amphibolites derived from boninites,
303 island arc tholeiites and picrites (Figs. 1 and 6; Gill et al., 1981; Polat et al., 2002; Polat
304 and Hoffman, 2003 and Appel et al., 2008), alluding to associations developed at a
305 convergent plate boundary.

306 4.3.2. Sample G04/54 of metacarbonate and chert in the northeast of the Isua
307 supracrustal belt. At the G04/54 locality (Fig. 1, GPS 65°10.760'N 49°48.153'W) in
308 the northeast end of the belt, a unit of metachert, carbonates and BIF cap a refolded
309 anticline of upward-facing pillowed metavolcanic rocks (these pillows were first
310 described by Solvang, 1999). These are both structurally overlain by a thrust sheet of
311 boninitic amphibolites (see Fig. 6 of Friend et al., 2007). The metacarbonate plus chert
312 sample G04/54 displays a REE+Y marine-like trace element signature, albeit the
313 abundances of total REE, Zr (13.5 ppm) and Al_2O_3 (1.72 wt%) are somewhat higher
314 than typical for such rocks. It is, therefore, interpreted as chemical sediment that was
315 moderately contaminated with a volcanic or detrital component (Friend et al., 2007).
316 G04/54 yielded twenty-eight prismatic zircon grains and fragments. In CL images the
317 majority of the grains are either non-luminescent or display complex recrystallisation
318 domains (Fig. 7). Therefore, only six grains with some relict oscillatory zoning were
319 dated (Table 1). Grains 1, 3 and 5 are assessed to have ages of ca. 3707, 3731 (two
320 analyses) and 3729 Ma, respectively. The other grains are much higher in U+Th, give
321 younger ages, and are interpreted to be disturbed.

322

323 4.3.3. Metachert samples G91/74 and 75 from the eastern end of the Isua supracrustal
324 belt. These are >2 kilogram samples from a large unit of metachert near the Inland Ice
325 (map position 65°12.33'N 49°47.87'W, Fig. 1). Whole rock analysis (Friend et al.,
326 2007) of G91/75 shows a well-developed REE+Y seawater-like signature, with very
327 low Zr (0.5 ppm) and Al_2O_3 (0.16 wt%) abundances, indicating it to be a pure
328 metachert with very little detrital input. Consequently, despite the larger sample sizes,
329 G91/74 yielded only seven zircons and G91/75 only six (Table 1). In G91/74, grains #2

and 3 with Mesoarchaean and Mesoproterozoic ages are interpreted as laboratory contaminants and they are considered no further. One of the remaining grains had high common Pb and was rejected. Of the remaining ten grains, one gave a low $^{207}Pb/^{206}Pb$ age of 3624 Ma (some radiogenic Pb loss?), and the others ranged in age from 3703 to 3677 Ma, but all still do not agree within analytical error (Table 1).

4.3.4. G07/07 BIF with the Rosing (1999) "early life" felsic schist unit. The felsic schists of the Rosing (1999) 'early life' unit in the northwest of the Isua supracrustal belt contain a BIF unit up to several metres thick (Maps 1 and 2 of Nutman and Friend, this volume). The BIF sample G07/07 was collected uphill to the south of the Rosing locality at GPS 65°08.654'N 50°10.114'W. It has moderate-low abundances of TiO_2 (0.12 wt%) and Al_2O_3 (3.25 wt%; Nutman and Friend, unpublished data), suggesting a moderate input from a non-chemical sedimentary source. It yielded a single, ca. 90 μm prismatic zircon. This showed some recrystallisation that disrupted oscillatory zoning parallel to the grain exterior (Fig. 8). Three analyses were undertaken and gave a weighted mean $^{207}Pb/^{206}Pb$ age of 3689±5 Ma.

4.3.5. G07/08 BIF within amphibolites of the 3700 Ma island arc tholeiite and picrite chemical affinity sub-terrane, northwest part of the belt. Amphibolites of the 3700 Ma juvenile island arc sub-terrane (Nutman and Friend, this volume), or the *inner arc unit* of Polat and Hofmann (2003), contain a north-south trending, laterally continuous (>10 km) metachert/BIF unit (Figs. 1 and 6; map in Nutman and Friend, this volume). This unit is highly deformed, with discontinuous layering entirely of tectonic origin and containing domains of rootless sheath folds. Thus, despite its obvious sedimentary protolith, it is now a meta-mylonite. Zircon dating of a southern occurrence of this unit (sample G93/19) was reported by Nutman et al. (2002, see below). Here we report zircon dating of sample G07/08 at another locality, at GPS 65°08.432'N 50°09.302'W (Figs. 1 and 6). It has low abundances of TiO_2 (<0.01 wt%) and Al_2O_3 (0.13 wt%; Nutman and Friend, unpublished data).The sample yielded 5 small prismatic zircons (Fig. 7). One was highly fractured, thus only four were analysed (Table 1). Grains #1, 3 and 4 gave $^{207}Pb/^{206}Pb$ ages of 3700-3680 Ma, and grain #5 gave an age of ca. 3750 Ma.

4.3.6. Previously analysed metacherts and BIF from the northern ca. 3700 Ma terrane. Zircon dating was reported on metachert/BIF samples G93/19, IEh50, G04/85 (Nutman et al. 2002, 2007a) and possible meta-conglomerate SM/GR/93/01 (Kamber et al. 2005). G93/19 (map position 65°5.8'N 50°8.8'W, Fig. 1, from the same unit as G07/08) yielded 4 small zircons suitable for analysis. Some of these have mantles of low Th/U recrystallised zircon or new growth, which are interpreted to have developed *in situ* during metamorphism. Three analyses entirely within such domains (#1.2, 2.3 and 4.1, Table 1) have ca. 3550 Ma ages, which gives the minimum time of deposition. The older zircons with oscillatory zoning gave ages of ca. 3725, 3706 and 3722 Ma (Table 1). BIF sample G04/85 with a seawater-like REE+Y signature and low Zr (0.6 ppm) and Al_2O_3 (0.19 wt%) (Friend et al., 2007) comes from the eastern end of the belt (Fig. 1, GPS 65°10.310'N 49°49.224'W). About 1 kilogram of this sample yielded three small oscillatory-zoned zircons, with grain #3 showing extensive recrystallisation domains (Fig. 7). Five analyses were undertaken (Table 1). A single analysis of partly recrystallised grain #3 yielded a low $^{207}Pb/^{206}Pb$ age of 3619 Ma, and is interpreted to have suffered some ancient loss of radiogenic Pb and is considered no further. Two analyses each of grains #1 and 2 yielded mean ages of 3700±12 and 3699±7 Ma respectively (Table 1). Sample IEh50ch (provided by S. Maruyama) from nearby in the same unit yielded nine oscillatory-zoned zircons, upon which ten analyses were undertaken (Table 1). All the ages of these grains agree within analytical error, yielding a weighted mean $^{207}Pb/^{206}Pb$ age of 3691±6 Ma (MSWD=1.0). Sample SM/GR/93/01 is from the same unit but on a fold limb to the south (Fig. 1), and is from a local lithological variant described as either a sedimentary conglomerate (e.g. Fedo, 2000) or as a carbonated tectonic breccia (e.g., Myers, 2001). Regardless of these diverse origins, this lithology is within a major unit of meta-chemical sedimentary rocks. Kamber et al. (2005) separated one zircon from SM/GR/93/01, for which two analyses give an age of 3740±7 Ma (Table 1). Thus these chemical sedimentary rocks show some zircons as young as ca. 3690 Ma, but none are >3750 Ma (Fig. 2a).

4.4. Northern ca. 3700 Ma terrane felsic and mica schists

4.4.1. The Rosing (1999) "early life evidence" felsic schist unit. This locality is at GPS 65°08.85'N 50°09.97'W (first found by the late Vic McGregor in 1973) in the northwest end of the Isua supracrustal belt (sample G05/28 on Figs. 1 and 6). The sample comes from a 50-100 m wide panel of quartzo-feldspathic and micaceous

schists that can be followed north-south for >1km. This panel also contains a BIF unit (sample G07/07, described above) which traverses obliquely across it. Description of these rocks and their interpretation as metasedimentary rocks was given by Nutman et al. (1984), Rosing (1999) and Fedo et al. (2001). The felsic schists and their associated BIF are strongly deformed and the panel is mylonite-bounded between amphibolite schists with boninitic chemistry to both the east and west. Understanding the age of these felsic schists is important, because ^{13}C-depleted graphite from them has been proposed as evidence of very early life (Rosing, 1999).

Samples G05/28 is a fine-grained and G05/29 is a coarser-grained quartzo-feldspathic schist (whole rock analyses in Table 1 of Nutman and Friend, this volume) are from ca. 10 m to the south and along strike from, the featured Rosing (1999) locality. Sampling was done this way to preserve the original Rosing site. In both G05/29 and G05/28, the main chlorite + biotite + muscovite foliation is concordant with gross lithological layering and is transgressed by a secondary chlorite-bearing cleavage. All fine-scale features of these rocks appear to be tectonic, with only the gross, metre-scale layering possibly representing transposed volcanic or sedimentary stratification. These felsic schists have compositional affinities with Archaean greenstone belt andesites or sedimentary rocks derived from such rocks, and their Nd isotopic compositions indicate a juvenile (volcanic?) provenance (Rosing et al., 1999; Nutman and Friend, this volume).

Three zircons were recovered from the combined mineral separation on about 1 kilogram of G05/28 and 29. Zircon #1 is a stubby, oscillatory-zoned, 35 μm prism with oscillatory zoning parallel to its margins (Fig. 8). Zircon #2 is a ca. 50 μm long fragment of a prism, with oscillatory zoning parallel to its margins but partly disrupted by recrystallisation domains. Zircon #3 is a ca. 50 μm prism that is somewhat duller in CL images, but still shows weak oscillatory zoning in CL images. No obvious outer shells of younger zircon could be seen on the grains (Fig. 8). All sites show high (>0.55) Th/U typical of igneous zircon (Table 1). Their habit, oscillatory zoning and Th/U suggest they are igneous, rather than metamorphic in origin. The lack of abrasion on the grains is in keeping with their being of volcano-sedimentary origin, rather than representing grains with a long residence time in a sedimentary system. Most analyses yielded close to concordant dates, with two dispersing to slightly younger ^{207}Pb/^{206}Pb ages (Table 1). Five analyses of these grains were undertaken on the SHRIMP-RG

instrument in the Australian National University, then after repolishing, an additional five analyses were undertaken on the BJSHRIMP in Beijing (Table 1). In this way duplicate analyses were achieved on all the grains. These grains might show slight real differences in their deduced ages of 3723±6 (grain #1) and 3724±6 (grain #2) versus 3712±2 Ma (grain #3).

4.4.2. The Harper and Jacobsen (1992) "^{142}Nd-anomaly" locality. This locality is at 65°12.04'N 49°48.16'W (GPS) in the northeast end of the Isua supracrustal belt, against the edge of the Inland Ice (sample G97/63 on Fig. 1). This position was given by Bob Dymek (personal communication, 1993) who collected sample IE715-28 from which Harper and Jacobsen (1992) reported the first terrestrial ^{142}Nd anomaly. We found evidence of previous sample collecting there, and we collected to duplicate it. The locality is within the same unit of andesitic to dacitic schists of volcanic or sedimentary origin that was previously dated along strike to the southwest as 3710-3700 Ma (Nutman et al., 1996, 1997). The reason for the extra sampling at this first reported terrestrial ^{142}Nd-anomaly site was to check for any extraneous ancient zircons which might be linked to the ^{142}Nd anomaly. In terms of lithology and state of deformation, the rocks sampled are very similar to those at the Rosing (1999) locality described above.

Sample G97/63 gave a moderate yield of zircons, all with oscillatory zoning and displaying little rounding. Seventeen analyses were undertaken on seventeen grains. Grain centres that had any possibility of being inherited cores were targeted to seek out any possible very old (Hadean) zircons. Grain #6 was rejected because its ages are too discordant, and grains #7 and 8 were also rejected (<3690 Ma) as candidates for ancient loss of radiogenic Pb. The ages of the remaining fourteen analyses agree within analytical error, with a weighted mean ^{207}Pb/^{206}Pb age of 3703±4 Ma (MSWD=0.9). Thus no anomalous old zircons were detected in this sample.

4.4.3. Previously dated northern ca. 3700 Ma felsic schists. Two groups of felsic schists were dated previously by zircon U/Pb methods. Running through the centre of the belt near the edge of the ca. 3800 Ma terrane is a felsic schist unit (on Fig. 1), from which oscillatory-zoned zircons of ca. 3800 Ma have been reported (Baadsgaard et al., 1984; Michard-Vitrac et al., 1977; Compston et al., 1986; Nutman et al., 2002, 2007a).

463 A variety of proposed origins for this unit include variably altered felsic volcanic rocks
464 (Allaart, 1976; Nutman et al., 1984), sheared altered tonalite (Rosing et al., 1996; Fedo
465 and Moorbath, 2005), and drastically-metasomatised amphibolite (Myers, 2001). A
466 detailed re-appraisal of this unit will be given elsewhere, but at this juncture we
467 observe that regardless of its origin, the zircon ages indicate an age for it and the
468 adjacent units of ≥3800 Ma, not 3700 Ma.

469 The northern parts of the Isua supracrustal belt contain felsic schists of broadly
470 andesitic, or more rarely, dacitic composition (from the same locality G91/76 and
471 G93/73 in Table 2 of Nutman and Friend, this volume). These are interlayered with
472 mafic schists containing garnet, biotite, chlorite and locally kyanite, cordierite or
473 staurolite, and like similar rocks at the Rosing (1999) 'early life' locality described
474 above (our samples G05/28 and 29), they are found in tectonic contact with boninitic
475 amphibolite units. The broad unit of these felsic rocks on the western side of the belt
476 against the Inland Ice (Fig. 1) is largely andesitic in composition and barren of zircons.
477 However on its eastern side there are rocks more evolved in composition, in which
478 relict graded clast structures are preserved (GPS 65°10.226'N 49°50.363'W),
479 indicative of a volcanic or volcano-sedimentary protolith (Nutman et al., 1997). These
480 rocks carry igneous oscillatory-zoned zircons (Nutman et al., 1996, 1997; Kamber et
481 al., 2005). Zircon results from a clast-free top of a unit (sample G91/76) and from a
482 clast-rich base of a unit (sample G93/75) were presented by Nutman et al. (1996, 1997)
483 and are reappraised here. For sample G91/76, twenty-four analyses were undertaken on
484 twenty-three grains (Nutman et al., 1996; Table 1), with a spread in near-concordant
485 $^{207}Pb/^{206}Pb$ dates of 3733-3603 Ma. These analyses were made in 1991 without
486 guidance of CL images, and probably include some disturbed domains, giving the
487 youngest apparent ages. This is supported by the duplicate analyses of grain #18 with
488 apparent $^{207}Pb/^{206}Pb$ ages of 3733 and 3660 Ma. Excluding the four youngest apparent
489 ages of <3690 Ma (the age of voluminous tonalites in the northern complex that are
490 younger than all supracrustal rocks) the remaining nineteen grains still do not form a
491 population with ages indistinguishable from each other (Table 1). For sample G93/75,
492 thirty-four analyses were undertaken on thirty-two zircons (Nutman et al., 1997).
493 Duplicate analyses of grain #25 were of a volcanic/detrital zircon. Grain #32 was
494 analysed on a volcanic/detrital core and a metamorphic rim, the latter with low Th/U
495 and a $^{207}Pb/^{206}Pb$ apparent age of 3504 Ma. The age of another low Th/U rim on grain
496 #17 is 3597 Ma. These rim analyses are not considered further here. The

volcanic/detrital zircons show a spread in apparent $^{207}Pb/^{206}Pb$ ages, even when those with ages of <3690 Ma are culled, as being the most likely candidates showing ancient loss of radiogenic Pb.

In the western part of the belt are more strongly deformed felsic schists, also intercalated with boninitic amphibolites and garnet-mica schists (sample G93/22, map position 65°5.5'N 50°8.4'W, Fig. 1). A <250 gram remnant was used for zircon separation, from which 5 zircons were obtained (Nutman et al., 1997). Grains 1, 2 and 4 appear to be variably disturbed late Archaean metamorphic zircons, and grain 5 is a Mesoproterozoic contaminant. None of these grains are considered further here. Three analyses on grain #3 yielded a weighted mean $^{207}Pb/^{206}Pb$ age of 3712±6 Ma (MSWD=0.1), identical to the youngest grain from felsic schist samples G05/28+29 to the north (above), that are also intercalated with boninitic amphibolites.

4.4.5. Previously-dated northern ca. 3700 Ma terrane garnet-mica schists. Garnet mica schists that mark the eastern edge of the major unit of felsic schists in the east of the belt carry mostly 3690-3730 Ma zircons (Fig. 1; see above). This schist unit has been interpreted as derived from weathered mafic rocks (Nutman et al., 1984; Kamber et al., 2005) but has interlayers of more felsic schists, like those described and dated above (G91/76, G93/73 and G97/63). Because of its predominantly mafic sedimentary provenance, few detrital zircons can be expected to occur within it. Nonetheless, Kamber et al. (2005) were successful in extracting a few small prismatic oscillatory zoned zircons from three samples of these schists (SM/GR/93/57, SM/GR/97/22 and 23; Fig. 1), with $^{207}Pb/^{206}Pb$ ages between 3718-3678 Ma, an age spread beyond that expected from analytical error alone (Table 1). Thus, these felsic volcanic and sedimentary rocks and mica schists show some zircons as young as 3690-3680 Ma, but none are >3750 Ma (Fig. 2b).

4.5. The dividing sedimentary unit

The dividing sedimentary unit runs the length of the Isua supracrustal belt and is highly tectonised, and in the central reaches of the belt it is considerably thinned on the limbs of early asymmetric folds, where locally it might be excised (see Maps 1 and 2 of Nutman and Friend, this volume). It has the singular feature of separating all the ca. 3700 Ma zircon age determinations in the north of the belt from all the ca. 3800 Ma age determinations to the south (Fig. 1).

Zircons from three samples (G93/28; G05/18; G07/22 – Figs. 1 and 9) of the dividing sedimentary unit were dated. Carbonate-bearing sample G93/28 (map position 65°05.63'N 50°10.45'W) has a well developed seawater-like REE+Y signature and quite low Zr (2.2 ppm) and Al_2O_3 (0.31 wt%) and is interpreted as a chemical sediment with only minor contamination from volcanic or detrital material (Friend et al., 2007). Ca. 500 grams of this sample yielded eight zircons. Of these, by far the largest grain is a laboratory contaminant. Thus, only results for the other 7 grains considered to belong to the rock are presented here (Table 1; Fig. 9). Four grains were large enough to undertake duplicate analysis. The data are assessed to show that there are five 3925-3875 Ma grains, one grain of possible ca. 3810 Ma age and one ca. 3750 Ma grain.

G07/22 (Figs. 1 and 6; GPS 65°08.059'N 50°11.464'W) is a ca. 1 kilogram sample and comprises three randomly selected pieces taken within 3 metres across strike of each other. This was done to increase the probability of obtaining zircons. It has <0.01 wt% TiO_2 and 0.19 wt% Al_2O_3 (Nutman and Friend, unpublished data) showing it contains very little volcanic or terrigenous detrital material. The sample yielded thirteen zircons, of which eleven were suitable for analysis (Fig. 9). One larger than average zircon is Palaeoproterozoic in age and different in character to the rest; it is undoubtedly a laboratory contaminant and is not considered further. Of the remaining ten, smaller zircons (Table 1), duplicate analyses were undertaken on grains #3, 4 and 8. The data are assessed to show that there are eight 3940-3850 Ma and two ca. 3750 Ma grains.

Sample G05/17 is of quartz-rich BIF from a low strain lithon in the eastern end of the belt (Fig. 1; GPS 65°09.869'N 49°48.936'W). About 500 grams of a sawn slab sample traversing several original sedimentary layers were used for zircon separation. It has 0.01 wt% TiO_2 and 0.16 wt% Al_2O_3 (Nutman and Friend, unpublished data) showing it contains very little volcanic or terrigenous detrital material. This sample yielded two tiny oscillatory zoned zircons (Fig. 9). The structurally best-preserved grain #1 has an age of 3771 ±16 Ma from one analysis. Two analyses of partly recrystallised grain #2 gave a mean age of 3742 ± 7 Ma. Grain #2 appears partly recrystallised in the CL image, and therefore its mean age is probably an underestimate of the true age. Thus, the youngest zircons in the dividing sedimentary unit are ca. 3750 Ma, but with more 3940-3880 Ma ones present (Fig. 2d).

At its western end, the dividing sedimentary unit is cut by a deformed granitic sheet approximately 0.5 m wide. The host metasedimentary rocks are much more strongly deformed, with layering now entirely of tectonic origin. Sample G07/20 of this granitic sheet (GPS 65°08.094'N 50°11.608'W – Fig. 6) yielded abundant prismatic zircons with widely preserved oscillatory zoning. CL images show that the zircons do not contain inherited cores and metamorphic rims, and thus they are regarded as a variably recrystallised simple igneous population. Some sites, particularly towards the grain exteriors, are high-U, and partly metamict with high common Pb (Table 1). Thus, sites show a spread in $^{207}Pb/^{206}Pb$ well beyond analytical error. If those with low $^{207}Pb/^{206}Pb$ are interpreted to have undergone some ancient loss of radiogenic Pb, then the remaining sites with low common Pb yield a weighted mean $^{207}Pb/^{206}Pb$ age of 3658±6 Ma. This is interpreted as the age of intrusion of this sheet. It is also the minimum age for the deposition and strong early deformation of the dividing sedimentary unit.

4.6. Southern ca. 3800 Ma terrane fuchsite quartzite

Along the borders of the ca. 3800 Ma felsic schist unit in the southern ca. 3800 Ma terrane there are intermittent, thin units of medium- to fine grained fuchsite quartzite associated with veins and layers of coarsely crystalline quartz-rich material of non-sedimentary origin. G93/25 from the western end of the belt was dated previously (map position 65°5.32'N 50°10.38"W Figs. 1 and 2; Nutman et al., 1997). The youngest concordant zircon (grain #27 with two analyses, Table 1) is ca. 3810 Ma, but most are older at 3900-3820 Ma (Fig. 2). This zircon population indicates that at least some of these quartzites (but not necessarily all) either have sedimentary protoliths or contain a detrital sedimentary input. The lack of <3800 Ma detrital zircons is in accord with ages of ca. 3800 Ma obtained on nearby sheets of tonalite that cut amphibolites in the southern side of the belt (Fig. 1; Nutman et al., 1996, 1997; Crowley, 2003).

4.7. Isua supracrustal belt metasedimentary rocks with some 3650-3600 Ma zircons?

Until now there has been a consensus from geochronology that all volcanic and sedimentary rocks in the Isua supracrustal belt have ages of ≥3700 Ma (e.g., Moorbath et al., 1973; Hamilton et al., 1978; Jacobsen and Dymek, 1987; Moorbath et al., 1997; Nutman et al., 1996, 1997, 2002, 2007a; Crowley, 2003; Kamber et al., 2005).

Therefore detrital zircons with ages as much as 100 million years younger than 3700 Ma have not been expected in the belt.

In the study of Nutman et al. (1997), sample 288626 (Fig. 1) from a 'dirty banded iron formation' within the northern ca. 3700 Ma terrane has some zircons with ages of ca. 3700 Ma, but also several other zircons have close to concordant ages >100 million years younger, to <3600 Ma (Table 1). Analysis of this sample was undertaken in the early 1990s without the benefit of CL imagery to choose the least recrystallised zircon domains. Therefore, it was regarded that some of these 'young' grains could be disturbed and to have lost some radiogenic Pb in ancient times. However, we now consider that this might be an incorrect appraisal of the data, and that the sample might really contain some zircons younger than 3700 Ma. This unit is along strike with a late Eoarchaean mylonite zone further north and west in the belt (Figs. 1, 6). Sample G07/27 of siliceous magnetite-bearing rock from this mylonite zone was collected at GPS 65°08.460'N 50°10.826'W. Approximately 1.5 kg of rock yielded 6 small zircons (in this case the mineral separation was at the Chinese Academy of Geological Sciences, Beijing). All grains are small, with variably-preserved oscillatory zoning (Fig. 10). Grain #3 gave early Palaeozoic ages (Table 1) and is clearly a laboratory contaminant. Grain #2 shows oscillatory zoning that is strongly disrupted by recrystallisation, and gave strongly discordant Palaeoproterozoic $^{207}Pb/^{206}Pb$ age. Two analyses of well-preserved oscillatory-zoned prism grain #1 gave a weighted mean $^{207}Pb/^{206}Pb$ age of 2557 ± 34 Ma. This is enigmatic. If it is truly a detrital grain belonging to this sediment and not a laboratory contaminant, then it would indicate a very young age of deposition. The remaining 3 zircons yield older ages. A single analysis of somewhat recrystallised grain #5 gave a $^{207}Pb/^{206}Pb$ age of 3630 Ma. Two analyses each on well-preserved prismatic grains #4 and #6 gave distinguishable weighted mean $^{207}Pb/^{206}Pb$ ages of 3697 ± 6 and 3717 ± 6 Ma, respectively.

From the central-southern part of the belt within the ca. 3800 Ma terrane, fuchsite-quartzite MR81-318 reported by Nutman and Collerson (1991) (Fig. 1; Google Earth reference 65°7.295'N 49°53.903'W from M. Rosing, written communication, 2008) has detrital zircons up to 3866 Ma, but also some grains of likely detrital origin that were appreciably younger (3700-3600 Ma), but still with close to concordant ages (Table 1). This sample is also a rarity, in that it has zircons with low Th/U Neoarchaean (ca. 2700 Ma) metamorphic overgrowths (grains #2, 3, 5 and 14, Table 1). As this was the first detrital zircon study published on the Isua

631 supracrustal belt, most attention was paid to finding the very old ≥3850 Ma detrital
632 components, and the interpretation and significance of the younger ages then took
633 lesser precedence.

634 In the southwest of the belt within the ca. 3800 Ma terrane, there is a thin (<10
635 m), but laterally continuous, unit of siliceous rocks that locally contains
636 magnetite-bearing BIF (Fig. 1). Further east this might link with a unit of similar
637 character in the southern part of the belt, for example where MR81-318 was sampled
638 (Fig. 1). This laterally-continuous unit clearly consists at least in part of mylonitised
639 metasediment with old (>3850 Ma) zircons (e.g., MR81-318), but it is unknown
640 whether the sedimentary component is continuous along it, or if it forms lenses along a
641 siliceous mylonite. Samples G07/02 and G07/04 are from this unit in the southwest of
642 the belt at 65°05.267'N 50°10.753'W (GPS). Here, the unit is <5 m wide and contains
643 magnetite, indicating some BIF is present. The two samples are from the north and
644 south sides of the unit, and were combined as a single mineral separation. Together
645 they have low abundances of TiO_2 (0.01 wt%) and Al_2O_3 (0.24 wt%; Nutman and
646 Friend, unpublished data). They yielded approximately 20 zircons, many of which are
647 larger (>100 μm long) than usual for chemical sedimentary rocks. In CL images, the
648 grains display oscillatory zoning parallel to the grain exteriors (Fig. 10). Several of the
649 grains have homogeneous non-luminescent CL image (dark) rims, which are too
650 narrow for analysis. The broadest of these was on grain #4 (Fig. 10). Many of the grains
651 show considerable partial recrystallisation. Eight analyses were undertaken on eight
652 grains. Seven analyses of seven grains (Fig. 10) all have close to concordant ages with
653 $^{207}Pb/^{206}Pb$ ages from 3898 to 3646 Ma, with four <3690 Ma (Table 1). An analysis of
654 the oscillatory-zoned core of grain #4 gave a $^{207}Pb/^{206}Pb$ age of only 2830 Ma. From an
655 analytical perspective, there are no grounds to reject this analysis. The only pretext
656 could be that it is a laboratory contaminant grain.
657
658 **5. Discussion**
659 *5.1. Interpretation of the very few zircons – resolving tectonic models for Isua*
660 Accurate U/Pb zircon dating of volcanic layers (commonly degraded into
661 clay-rich materials – tonsteins) is a key technique for quantifying the Phanerozoic to
662 Palaeoarchaean timescale. The assessment of these zircon ages is always fraught with a
663 dilemma: For a non-Gausian age spectrum, to what extent is the extra dispersion due to
664 subtle ancient loss of radiogenic Pb, and to what extent is it due to the incorporation of

detrital grains only a million or so years older than the volcanic depositional event? Extracting the age of deposition from the few zircons in the Isua chemical sedimentary rocks and the larger number of zircons in the dacitic or more acidic volcanic rocks faces similar problems, and it would be unrealistic to fix the maximum ages of deposition to <±10 million years. This uncertainty is displayed in Figure 2. However two findings are abundantly clear from the Isua supracrustal belt sedimentary zircon age data, which transcend these problems.

First, the age of youngest zircons in the different sedimentary units is different (Fig. 2): ca. 3810 Ma for the fuchsite quartzite G93/25 in southern terrane; ca. 3750 Ma for three samples of the dividing metasedimentary unit (G93/28, G05/17 and G07/22); 3700-3690 Ma for the more numerous chemical sediment samples from the northern terrane. These data make it extremely unlikely that any of these units are tectonic repetitions of the same stratigraphic layer by either folding or thrusting.

This is further evidence against the stratigraphic scheme erected for the belt from mapping in the early 1980s (Nutman et al., 1984) that was abandoned by Nutman et al. (1997). In such a stratigraphic scheme, the unit of chemical sedimentary rocks containing samples G91/74, G91/75, G04/85, IEh50ch and G04/54 would have been considered to be a lateral equivalent of the dividing sedimentary unit represented by G93/28, G05/17 and G07/22 as a unit designated as 'A4' in the early 1980s interpretation. It is also incompatible with the interpretation of the Isua supracrustal belt representing a single accretionary complex, in which all chemical sedimentary units are stratigraphically equivalent tectonic repetitions from an oceanic chemical sedimentary unit capping basalts within an ocean plate stratigraphy (see Maruyama et al., 1992; Komiya et al., 1999). Thus our results support a model of juxtaposition of separate terranes, unrelated to each other and formed at different times (Figs. 2 and 3).

Second, the age of the youngest volcanic and sedimentary zircons in the northern ca. 3700 Ma terrane is surprisingly young, at 3700-3690 Ma, statistically younger than the ages of 3717-3712 Ma tonalite sheets that invade metavolcanic amphibolites adjacent to these units (Figs. 2 and 6; Grimes and Dunning, 2002; Nutman and Friend, unpublished data). The implication from this is that these chemical sedimentary rocks are either tectonic intercalations within slightly older arc-related mafic volcanic sequences, or that the sedimentary rocks were deposited on top of the metabasaltic amphibolites and were then tectonically intercalated at <3690 Ma. Thus a Phanerozoic analogue for these chemical sediments could volcanic

ash-bearing radiolarian cherts that overlie upper volcanic series rocks in some arc/ophiolite volcanic assemblages (e.g., Page 1972). On the other hand, the ca. 3690-3700 Ma ages of these zircons does match that of other slightly younger tonalites that dominate the ca. 3700 assemblage (Fig. 2). These tonalites, or perhaps coeval dacites, might have been the source of the 3700-3690 Ma detrital zircons in these metasedimentary rocks.

5.2. *Juvenile nature of the ca. 3700 Ma terrane*

Within the ca. 3700 Ma northern terrane felsic metavolcanic and the chemical metasedimentary rocks there are a few zircons as old as 3750-3740 Ma, some others with ages of 3730-3710 Ma and most 3710-3680 Ma (Fig. 2). However, *no* >3750 Ma zircons have been detected in any rock, despite the fact that just to the south lies an extensive terrane of largely ca. 3800 Ma rocks (Fig. 1; Nutman et al., 1996, 1997, 2002). Clearly then, ≥3800 Ma detritus from this southern terrane was not being fed into the ca. 3700 Ma volcanic and sedimentary environment now preserved in the northern terrane. The simplest explanation of this is that the northern ca. 3700 Ma terrane contains juvenile arc rocks that formed *remote* from the older ca. 3800 Ma southern terrane, until they collided sometime after 3690 Ma (Fig. 2). Such an interpretation is in accord with the island arc-like geochemistry of the northern 3700 Ma amphibolites (Polat et al. 2002; Polat and Hoffman, 2003) and the juvenile Nd isotopic signatures of the northern rocks (e.g., data within Hamilton et al., 1978; Jacobsen and Dymek, 1987; Gruau et al., 1996 and Moorbath et al., 1997).

5.3. *Significance of zircon dates from the dividing sedimentary unit*

The dividing sedimentary unit has its own distinctive detrital zircon age signature (Fig. 2). All three dated samples have youngest zircons at ca. 3750 Ma, which give a maximum age of deposition for this unit. Two samples with the most grains (G93/28 and G07/22) have more grains with 3940-3880 Ma ages. These are distinct from, and clearly older than, the extensive ca. 3800 Ma rocks in the terrane to the south. In fact, the 3940-3900 Ma zircons are the oldest dated grains from the Itsaq Gneiss Complex, but with no extant rocks of that age having been detected yet.

At some localities, the boundary of the dividing sedimentary unit and the ca. 3700 terrane to the north is unquestionably an early tectonic contact (Myers, 2001;

Nutman et al., 2002). Therefore we interpret the dividing sedimentary unit as package of predominantly chemical sedimentary rocks that were probably deposited on top of an already deformed 3800 Ma terrane (Fig. 3). The >3800 Ma detrital components within the dividing sedimentary unit were from a yet unidentified source, but probably connected with the ca. 3800 Ma terrane. We suggest that the dividing sedimentary unit acted as a décollement when the ca. 3700 Ma arc complex to the north docked with the southern ca. 3800 Ma terrane at 3690-3660 Ma (Figs. 2 and 3), as is discussed in Nutman and Friend (this issue).

5.4. Older crustal components in the ca. 3800 Ma terrane

Fuchsite-quartzite G93/25 in the ca. 3800 Ma complex contains predominantly 3900-3820 Ma detrital zircons (Nutman et al., 1997). Although rocks of this age are unknown from the Isua area, a crustally-derived granite from a few kilometres south of Isua contains a ca. 3850 Ma zircon xenocryst (sample G97/92 of Friend and Nutman, 2005), whereas further south in the Itsaq Gneiss Complex, there are now several localities with ≥3840 Ma tonalites, that occur together with ca. 3800 and ca. 3750 Ma tonalites (Nutman et al., 2000; 2007b). This suggests that the ca. 3800 Ma terrane is not entirely juvenile, but contains some components of older sialic crust.

5.6. Post-assembly sedimentary rocks and tectonism

Review of previously published zircon age data on two metasedimentary rocks MR81-318 and GGU288626, plus the data on G07/02+04 presented here, suggests that there are thin, highly tectonised siliceous units in the Isua supracrustal belt, which contain some zircons younger than 3660 Ma, the time by which the ca. 3800 and 3700 Ma terranes had already docked (Crowley, 2003). One possibility is that some mylonites with lenses of sedimentary rocks formed during or shortly after the docking of the ca. 3800 and 3700 Ma terranes. This would be in accord with zircon geochronology combined with detailed structural studies which indicate that important imbrication of unrelated rocks of different age and origin occurred at 3650-3600 Ma in and around the Isua supracrustal belt (e.g., Crowley et al., 2002; Nutman et al., 2002).

Infolding and imbrication of somewhat younger sedimentary rocks within Archaean accretionary orogens has been noted elsewhere, for example during the post accretionary ca. 2630 Ma Wangkatha Orogeny in the Yilgarn Craton, Western

765 Australia (Blewett et al., 2004). An alternative possibility is that the Isua supracrustal
766 belt acted as a locus for further deformation during later Archaean terrane assembly
767 (e.g. Friend and Nutman, 2005; Nutman and Friend, 2007), during which slivers of
768 younger Archaean sediment were incorporated along Neoarchaean mylonites. In which
769 case a single ca. 2840 Ma zircon in sample G07/02+04 could be a genuine detrital grain
770 rather than a laboratory contaminant. Sample MR81-318 has zircons with
771 Neoarchaean low Th/U metamorphic rims (Nutman and Collerson, 1991; Table 1);
772 Neoarchaean metamorphic zircons are very rare in the Isua supracrustal belt. Clearly,
773 the age of deposition of sedimentary components in these siliceous units is as yet
774 uncertain and warrants further investigation.
775
776 **6. Conclusions**
777 (1) Rare zircons from chemical metasedimentary rocks of the Eoarchaean Isua
778 supracrustal belt are of volcanic and sedimentary origin, and thereby provide
779 information on the age provenance of detritus and the maximum age of deposition
780 (Fig. 2).
781 (2) The age signatures for different sedimentary units varies: Metasedimentary rocks
782 associated with, and bounding, the ca. 3800 Ma southern terrane contain older detritus
783 back to ca. 3940 Ma. This demonstrates that either this southern terrane was not
784 entirely juvenile crust, or, there was an input of detritus derived from older unidentified
785 crust. Metasedimentary rocks associated with the northern ca. 3700 Ma terrane have
786 largely juvenile provenance, with the oldest, rare zircons 3750-3740 Ma old, and most
787 zircons are younger at 3720-3690 Ma (Fig. 2).
788 (3) Because of the different ages of zircons extracted from the Isua chemical
789 metasedimentary rocks, they cannot be regarded as tectonic slivers derived from a
790 single sedimentary unit, but instead are interpreted as derived from unrelated
791 juxtaposed assemblages (Fig. 3). This is further evidence against interpreting the Isua
792 supracrustal belt to contain a single accretionary complex, as was proposed by Komiya
793 et al. (1999).
794 (4) In the dividing sedimentary unit that occurs between the ca. 3800 and 3700 Ma
795 terranes the youngest detrital zircons are ca. 3750 Ma, giving the maximum age of
796 deposition. Map data suggest that it was deposited unconformably upon or tectonically
797 juxtaposed against, already folded and/or tectonically imbricated ca. 3800 Ma rocks of
798 the southern terrane.

(5) Some of the post-assembly tectonic breaks in the Isua supracrustal belt might contain slivers of post-assembly sedimentary rocks, which contain some zircons as young as ca. 3600 Ma. The age of these metasedimentary rocks and when they were imbricated with the already assembled 3800 and 3700 Ma terranes can only be resolved by further work.

Acknowledgments

1991-1997 support was via block funding from the Research School of Earth Sciences (RSES) of the Australian National University. For this we would particularly like to thank Bill Compston. There was logistical support and help in the field over several years from Ole Christiansen of Nunaminerals A/S and Minik Rosing of the Geological Museum of Copenhagen. On occasions this has been invaluable. We thank Peter Appel and the Isua Multidisciplinary Project for donating some helicopter time in 1997. From 2003 to 2005 support was via Australian Research Council grant DP0342794. Since 2006, laboratory and fieldwork support was via internal funding of the Chinese Academy of Geological Sciences. Shigenori Maruyama kindly provided metachert sample IEh50ch for SHRIMP dating. We thank Liu Dunyi for access to BJSHRIMP for many of the new analyses reported here. Finally we acknowledge many of our colleagues for discussions about Isua geology over the years, particularly Vickie Bennett, Minik Rosing and the late Vic. McGregor. The manuscript was greatly improved by thoughtful reviews by Ali Polat and Martin van Kranendonk.

References

Allaart, J.H., 1976. The pre-3760 m.y. old supracrustal rocks of the Isua area, central West Greenland, and the associated occurrence of quartz-banded ironstone. In: B.F. Windley (Editor), The Early History of the Earth. Wiley, London, pp. 177-189.

Appel, P.W.U., Polat, A., Frei, R., 2008. Dacitic ocelli in mafic lavas, 3.8-3.7 Ga Isua greenstone belt, West Greenland: Geochemical evidence for partial melting of oceanic crust and magma mixing, Chemical Geology, doi: 10.1016/j.chemgeo.2008.09.011.

Baadsgaard, H., Nutman, A.P., Bridgwater, D., McGregor, V.R., Rosing, M., Allaart, J.H., 1984. The zircon geochronology of the Akilia association and the Isua supracrustal belt, West Greenland. Earth Planetary Science Letters 68, 221-228.

Bennett, V.C., Brandon, A.D., Nutman, A.P., 2007. Hadean mantle dynamics from coupled 142-143 neodymium isotopes in Eoarchaean rocks. Science, 318, 1907-1910.

Blewett, R.S., Kassidy, K.F., Champion, D.C., Henson, P.A., Goleby, B.S., Jones, L., Groenewald, P.B., 2004. The Wangkathaa Orogeny: an example of episodic regional 'D_2' in the late Archaean Eastern Goldfields Province, Western Australia. Precambrian Research, 130, 139-159.

Bolhar, R., Kamber, B.S., Moorbath, S., Fedo, C.M., Whitehouse, M.J. 2004. Characterisation of early Archaean chemical sediments by trace element signatures. Earth and Planetary Sciences Letters, 222, 43-60.

Bohlar, R., Kamber, B.S., Moorbath, S., Whitehouse, M.J., Collerson, K.D., 2005. Chemical characterization of earth's most ancient clastic metasediments from the Isua. Geochimica et Cosmochimica Acta, 69, 1553-1573.

Caro, G., Bourdon, B., Birk, J.-L., Moorbath, S., 2003. ^{146}Sm–^{142}Nd evidence from Isua metamorphosed sediments for early differentiation of the Earth's mantle. Nature, 423, 428-430.

Compston, W., Kinny, P.D., Williams, I.S., Foster, J.J., 1986. The age and lead loss behaviour of zircons from the Isua supracrustal belt as determined by ion microprobe. Earth Planetary Science Letters 80, 71-81.

Crowley, J.L., 2003. U-Pb geochronology of 3810-3630 Ma granitoid rocks south of the Isua greenstone belt, southern West Greenland. Precambrian Research 126, 235-257.

Crowley, J.L., Myers, J.S., Dunning, G.R., 2002. Timing and nature of multiple 3700-3600 Ma tectonic events in intrusive rocks north of the Isua greenstone belt, southern West Greenland. Geological Society of America Bulletin 114, 1311-1325.

Dymek, R.F. and Klein, C., 1988. Chemistry, petrology and origin of banded iron-formation lithologies from the 3800 Ma Isua supracrustal belt, west Greenland. Precambrian Research, 39, 247-302.

Fedo, C.M., 2000. Setting and origin of problematic rocks from the >3.7 Ga Isua greenstone belt, southern West Greenland: Earth's oldest coarse clastic sediments. Precambrian Research 101, 69-78.

Fedo, C.M., Moorbath, S., 2005. Conglomerate or deformed and metasomatised tonalite? Geochemical evidence on the origin of the "boulder bed", Isua greenstone belt, Greenland. Geological Society of America 2005 annual meeting. Geological Society of America Abstracts with Programs, 37, page 386.

Fedo, C.M., Myers, J.S., Appel, P.W.U., 2001. Depositional setting and paleogeographic implications of Earth's oldest supracrustal rocks, the >3.7 Ga Isua Greenstone Belt, West Greenland. Sedimentary Geology, 141-142, 61-77.

Frei, R. and Polat, A., 2005. Source heterogeneity for the major components of ~3.7 Ga Banded Iron Formations (Isua Greenstone Belt, Western Greenland): Tracing the nature of interacting water masses in BIF formation. Earth and Planetary Science Letters, 253, 266-281.

Friend, C.R.L., Nutman, A.P. 2005. Complex 3670-3500 Ma orogenic episodes superimposed on juvenile crust accreted between 3850-3690 Ma, Itsaq Gneiss Complex, southern West Greenland. Journal Geology 113, 375-398.

Friend, C.R.L., Nutman, A.P., Bennett, V.C., Norman, M.D., 2007. Seawater-like trace element signatures (REE+Y) of Eoarchaean chemical sedimentary rocks from southern West Greenland, and their corruption during high grade metamorphism. Contributions to Mineralogy and Petrology, DOI 10.1007/s00410-007-0239z.

Gill, R.C.O., Bridgwater, D., Allaart, J.H., 1981. The geochemistry of the earliest known basic metavolcanic rocks, West Greenland: a preliminary investigation. Spec. Pub. Geol. Soc. Australia 7, 313-325.

Grimes, S.W., Dunning, G.R., 2002. A 3714 Ma pluton intruding the Isua greenstone belt, southwest Greenland; the world's oldest volcano-sedimentary section (or, at least part of it) gets older. Geological Society of America 2002 annual meeting. Geological Society of America Abstracts with Programs, 34, page 365.

Gruau, G., Rosing, M., Bridgwater, D., Gill, R.C.O., 1996. Resetting of Sm-Nd systematics during metamorphism of >3.7 Ga rocks: implications for isotopic models of early Earth differentiation. Chemical Geology, 133, 225-240.

Hamilton, P.J., O'Nions, R.K., Evensen, N.H., Bridgwater, D., Allaart, J.H., 1978. Sm-Nd isotopic investigations of Isua supracrustals and implications for mantle evolution. Nature, 272, 41-43.

Harper, C.L., Jacobsen, S.B., 1992. Evidence from coupled ^{147}Sm-^{143}Nd and ^{146}Sm-^{142}Nd systematics for very early (4.5 Gyr) differentiation of the Earth's mantle. Nature, 360, 728-732.

Hiess, J., Bennett, V.C., Nutman, A.P., Williams, I.S., in press. In situ U-Pb, O and Hf isotopic compositions of zircon from Eoarchaean tonalite and felsic volcanic rocks, Itsaq Gneiss Complex, southern West Greenland: New constraints on the source materials for the early crust. Geochimica et Cosmochimica Acta.

Jacobsen, S.B., Dymek, R.F., 1987. Nd and Sr isotope systematics of clastic metasediments from Isua, West Greenland: Identification of pre-3.8 Ga differentiated crustal components. Journal of Geophysical Research, 93, 338-354.

Kamber, B.S., Moorbath, S., Whitehouse, M.J., 2001. The oldest rocks on Earth: time constraints and geological controversies. Geological Society, London, Special Publication 190, 177-203.

Kamber, B.S., Whitehouse, M.J., Bolhar, R., Moorbath, S., 2005. Volcanic resurfacing and the early terrestrial crust: Zircon U-Pb and REE constraints from the Isua Greenstone Belt, southern West Greenland. Earth and Planetary Science Letters, 240, 276-290.

Komiya, T., Maruyama, S., Masuda, T, Appel., P.W.U., Nohda, S., 1999. The 3.8-3.7 Ga plate tectonics on the Earth; Field evidence from the Isua accretionary complex, West Greenland. Journal Geology 107, 515-554.

Keto, L., Kurki, J., 1967. Report on the exploration activity at Isua 1967. Kryolitselskabet Øresund A/S Prospektering report lodged as report 20024 at the Geological Survey of Denmark and Greenland.

Ludwig, K., 2003. Isoplot/Ex. Berkeley Geochronology Center, Publication 1

Maruyama, S., Masuda, T., Nohda, S., Appel, P., Otofuji, Y., Miki, M., Shibata, T., Hagiya, H., 1992. The 3.9-3.8 Ga plate tectonics on the Earth: Evidence from Isua, Greenland. Paper presented at the Evolving Earth Symposium, Tokyo Inst of Technol, Okazaki, Japan.

McClennan, S.M., 1989. Rare earth elements in sedimentary rocks: Influence of provenance and sedimentary processes. In Geochemistry and Mineralogy of Rare Earth Elements (eds. B.R. Lipinand and G.A. McKay), pp.169-200. Mineralogical Society of America.

Michard-Vitrac, A., Lancelot, J., Allègre, C.J., Moorbath, S., 1977. U-Pb ages on single zircons from the early Precambrian rocks of West Greenland and the Minnesota River Valley. Earth and Planetary Sciences Letters, 35, 449-453.

Mojzsis, S.J., Arrhenius, G., McKeegan, K.D., Harrison, T.M., Nutman, A.P. and Friend, C.R.L., 1996. Evidence for life on Earth before 3800 million years ago. Nature, 270: 43-45.

Moorbath, S., O'Nions, R.K., Pankhurst, R.J., Gale, N.H., McGregor, V.R., 1972. Further rubidium-strontium age determinations on the very early Precambrian rocks of the Godthåb district: West Greenland. Nature 240, 78-82.

929 Moorbath, S., Whitehouse, M.J., 1996. Age of the Isua supracrustal sequence of West
930 Greenland: A plausible repository for early life. InChels-Flores, J., Raulin, F. (eds.),
931 Chemical Evolution: Phyusics of the Origin of Life. Luwer, Dordrecht, pp. 87-95.
932 Moorbath, S., O'Nions, R.K., Pankhurst, R.J., 1973. Early Archaean age for the Isua iron
933 formation, West Greenland. Nature 245, 138-139.
934 Moorbath, S. Whitehouse, M.J., Kamber, B.S., 1997. Extreme Nd-isotope heterogeneity in
935 the early Archaean - fact or fiction? Case histories from northern Canada and West
936 Greenland. Chemical Geology 135, 213-231.
937 Myers, J.S., 2001. Protoliths of the 3.8–3.7 Ga Isua greenstone belt, West Greenland.
938 Precambrian Research 105, 129-141.
939 Nutman, A.P., 1986. The early Archaean to Proterozoic history of the Isukasia area, southern
940 West Greenland. Grønlands geologiske Undersøgelse Bulletin, 154, 80 pp.
941 Nutman, A.P., Collerson, K.D., 1991. Very early Archean crustal-accretion complexes
942 preserved in the North Atlantic Craton. Geology 19, 791-794.
943 Nutman, A.P., Friend, C.R.L. 2007. Adjacent terranes with ca. 2715 and 2650 Ma
944 high-pressure metamorphic assemblages in the Nuuk region of the North Atlantic
945 Craton, southern West Greenland: Complexities of Neoarchaean collisional orogeny.
946 Precambrian Research, 155, 159-203.
947 Nutman, A.P., Friend, C.R.L., this volume. New 1:20,000 geological maps, synthesis and
948 history of investigation of the Isua supracrustal belt and adjacent orthogneisses,
949 southern West Greenland: A glimpse of Eoarchaean crust formation and orogeny.
950 Precambrian Research, xxx, yyy-zzz.
951 Nutman, A.P., Friend, C.R.L., Bennett, V.C., 2002. Evidence for 3650-3600 Ma assembly of
952 the northern end of the Itsaq Gneiss Complex, Greenland: Implication for early
953 Archean tectonics. Tectonics, 21, article 5
954 Nutman, A.P., Bennett, V.C., Friend, C.R.L., Rosing, M.T., 1997. ~3710 and ≥3790 Ma
955 volcanic sequences in the Isua (Greenland) supracrustal belt; structural and Nd isotope
956 implications. Chemical Geology 141, 271-287.
957 Nutman, A.P., Friend, C.R.L., Bennett, V.C., McGregor, V.R., 2000. The early Archaean
958 Itsaq Gneiss Complex of southern West Greenland: The importance of field
959 observations in interpreting dates and isotopic data constraining early terrestrial
960 evolution. Geochimica et Cosmochimica Acta 64, 3035-3060.

961 Nutman, A.P., Allaart, J.H., Bridgwater, D. Dimroth, E., Rosing, M.T., 1984. Stratigraphic
962 and geochemical evidence for the depositional environment of the early Archaean Isua
963 supracrustal belt, southern West Greenland. Precambrian Research 25, 365-396.
964 Nutman, A.P., McGregor, V.R., Friend, C.R.L., Bennett, V.C., Kinny, P.D., 1996. The Itsaq
965 Gneiss Complex of southern West Greenland; the world's most extensive record of
966 early crustal evolution (3900-3600 Ma). Precambrian Research 78, 1-39.
967 Nutman, A.P., Friend, C.R.L., Horie, H., Hidaka, H., 2007a. Construction of pre-3600 Ma
968 crust at convergent plate boundaries, exemplified by the Itsaq Gneiss Complex of
969 southern West Greenland. *In:* van Kranendonk, M.J., Smithies, R.H., & Bennett, V.C.
970 (eds) *Earth's Oldest Rocks*. Elsevier, pp.187-218.
971 Nutman, A.P., Bennett, V.C., Friend, C.R.L., Horie, K., Hidaka, H., 2007b. C. 3850 Ma
972 tonalites in the Nuuk region, Greenland: Geochemistry and their reworking within an
973 Eoarchaean gneiss complex. Contributions to Mineralogy and Petrology, DOI
974 10.1007/s00410-007-0199-3.
975 Paces, J.B., Miller, J.D. Jr., 1993. Precise U-Pb ages of Duluth Complex and related mafic
976 intrusions, northeastern Minnesota: Geochronological insights to physical,
977 petrogenetic, paleomagnetic, and tectonomagmatic processes associated with the 1.1
978 Ga midcontinent rift system. J. Geophys. Res. 98, 13997–140013.
979 Page, B.M., 1972. Oceanic crust and mantle fragment subduction complex near San Luis
980 Obispo, California. Geological Society of America Bulletin 83, 957-971.
981 Pickard, A.L. 2003. SHRIMP U/Pb zircon ages for the Palaeoproterozoic Kuruman Iron
982 Formation, Northern Cape Province, South Africa; evidence for simultaneous BIF
983 deposition on Kaapvaal and Pilbara cratons. Precambrian Research, 125, 275-315.
984 Polat, A., Hofmann, A.W., 2003. Alteration and geochemical patterns in the 3.7-3.8 Ga Isua
985 greenstone belt, West Greenland. Precambrian Research 126, 197-218.
986 Polat, A., Hofmann, A.W., Rosing, M.T., 2002. Boninite-like volcanic rocks in the 3.7-3.8
987 Ga Isua greenstone belt, West Greenland: implications for post-magmatic alteration
988 processes. Geochimica et Cosmochimica Acta, 67, 441-457.
989 Rosing, M.T., 1999. ^{13}C-depleted carbon microparticles in >3700 Ma sea-floor sedimentary
990 rocks from West Greenland. Science, 283, 674-676.
991 Rosing, M.T., Rose, N.M., Bridgwater D., Thomsen, H.S., 1996. Earliest part of Earth's
992 stratigraphic record: a reappraisal of the ≥3.7 Ga Isua (West Greenland) supracrustal
993 sequence. Geology, 24, 43-46.

994 Sircombe, K.N., Bleeker, W., Stern, R.A., 2001. Detrital zircon geochronology and
995 grain-size analysis of a ~2800 Ma Mesoarchean proto-cratonic cover succession, Slave
996 Province, Canada. Earth and Planetary Science Letters, 189, 207-220.
997 Solvang, M., 1999. An investigation of metavolcanic rocks from the eastern part of the Isua
998 greenstone belt, Western Greenland. Geological Survey of Denmark and Greenland
999 (GEUS) Internal Report, Copenhagen, Denmark, 62 pages.
1000 Stern, R.A., 1998. High-resolution SIMS determination of radiogenic trace-isotope ratios in
1001 minerals. In L. J. Cabri and D.J. Vaughan (Editors). Modern approaches to ore and
1002 environmental mineralogy. Mineralogical Association of Canada Short Course Series,
1003 27, 241-268.
1004 Williams, I.S., 1998. U-Th-Pb geochronology by ion microprobe. In Applications of
1005 microanalytical techniques to understanding mineralizing processes. In: M.A.
1006 McKibben, W.C.P. Shanks III and W.I. Ridley (Editors). Soc. Econ. Geol. Short
1007 Course Vol. 7.
1008

Table captions

Table 1. Zircon SHRIMP U-Pb dates from Isua supracrustal belt sedimentary rocks. Sources for those published previously are given in the footnotes.

Table 2. Zircon Laser Ablation ICPMS trace element analyses for zircons in metacherts G91/75 and IEh50ch. $^{207}Pb/^{206}Pb$ ages are uncorrected for minor amounts of common Pb. See Nutman and Friend (2007) for analytical method.

Figure captions

Figure 1. Summary geological map of the Isua area, Nuuk region, southern West Greenland. Inset shows the location of the Isua area at the northern end of the Itsaq gneiss complex. Location of the discussed samples is shown.

Figure 2. Summary of zircon age data from Isua supracrustal belt sedimentary and volcanic rocks. Also shown is the likely maximum age of deposition for each group of sedimentary rocks, and the ages of tonalite sheets (from Nutman et al., 1997, 2002; Crowley, 2003; Grimes and Dunning, 2002 and Nutman and Friend, unpublished data). The *minimum* age of assembly of the northern and southern terranes is shown as 3660 Ma, the age of a distinctive suite of composite ultramafic, dioritic and granitic intrusions known as the Inaluk dykes that are common to both terranes (Crowley et al., 2002; Crowley, 2003; Friend and Nutman, 2005). Note that some tectonised siliceous units interpreted to contain siliceous metasediment have detrital zircons younger than this.

Figure 3. Cartoon sections depicting the evolution of Isua from ca. 3760 Ma to 3600 Ma.

Figure 4. PAAS normalised (McLennan, 1989) REE+Y patterns for Isua chert, BIF and sedimentary carbonate rocks (data from Friend et al., 2007).

Figure 5. Chondrite normalised Laser Ablation ICPMS rare earth element data for zircons in metacherts G91/75 and IEh50ch (see Nutman and Friend, 2007 for analytical method). Note the negative Eu anomaly in most of the analyses with low light REE abundance.

Figure 6. Geological map of field relations in the western end of the Isua supracrustal belt. This map is extracted from the 1:20,000 Isua solid geology Map 2 of Nutman and Friend (this

volume). Please note that the coordinates are from the Nutman (1986) 1:40,000 geological map. These coordinates do not coincide with the WGS84 datum used in GPS sample positions from 1997 onwards.

Figure 7. Cathodoluminescence images of dated zircons from metasedimentary rocks in the northern ca. 3700 Ma terrane. Analytical errors on the $^{207}Pb/^{206}Pb$ ages are given at the 1σ level.

Figure 8. Cathodoluminescence (CL), back scattered electron (BSE) and transmitted light images of dated zircons from felsic schist sample G05/28 + 29 in the northern ca. 3700 Ma terrane. Analytical errors on the $^{207}Pb/^{206}Pb$ ages are given at the 1σ level.

Figure 9. Cathodoluminescence images of dated zircons from dividing sedimentary unit samples. Analytical errors on the $^{207}Pb/^{206}Pb$ ages are given at the 1σ level.

Figure 10. Cathodoluminescence images of dated zircons from mylonitised siliceous units that might contain <3650 Ma metasediment. Analytical errors on the $^{207}Pb/^{206}Pb$ ages are given at the 1σ level.

Table 1: SHRIMP U/Pb zircon analyses

Site	Grain/site type	Assessed/filtered 207Pb/206Pb grain age (Ma)	U ppm	Th ppm	Th/U	comm. 206Pb%	238U / 206/Pb ratio	207Pb / 206Pb ratio	207Pb/206Pb site date (Ma)	conc (%)
1. Northern ca. 3700 Ma terrane										
1.1. Meta-chemical sediments with minor detrital/volcanic components										
1.1.1. new data										
G04/54 metacarbonate capping pillowed volcanic rocks, eastern part of the belt										
1.1	m,osc,eq	3707 ± 10	394	267	0.68	0.19	1.375 ± 0.063	0.3499 ± 0.0023	3707 ± 10	95
2.1	m,osc,p	3662 ± 52	960	549	0.57	0.21	1.401 ± 0.062	0.3399 ± 0.0114	3662 ± 52	95
3.1	m,osc,p	wm 3731 ± 14	88	51	0.58	0.30	1.235 ± 0.073	0.3555 ± 0.0046	3731 ± 20	103
3.2	m,osc,p		114	67	0.58	0.16	1.341 ± 0.070	0.3555 ± 0.0046	3731 ± 20	96
4.1	e,osc,p		1496	970	0.65	0.23	1.471 ± 0.034	0.3110 ± 0.0011	3526 ± 5	95
5.1	m,osc,p,fr	3729 ± 47	260	162	0.62	0.07	1.235 ± 0.070	0.3552 ± 0.0107	3729 ± 47	103
6.1	e,osc,p		1817	1649	0.91	0.24	1.683 ± 0.044	0.2694 ± 0.0012	3303 ± 7	91
***G91/74 metachert, eastern end of the belt**										
1.1	osc,p	3624 ± 12	270	216	0.80	2.41	1.292 ± 0.043	0.3316 ± 0.0026	3624 ± 12	101
2.1	*contaminant*		*1061*	*112*	*0.11*	*0.08*	*1.663 ± 0.054*	*0.235 ± 0.001*	*3088 ± 5*	*98*
3.1	*contaminant*		*630*	*327*	*0.52*	*0.20*	*4.240 ± 0.137*	*0.101 ± 0.001*	*1648 ± 20*	*83*
4.1	osc,p	o 3681 ± 5	357	113	0.32	0.09	1.315 ± 0.043	0.3441 ± 0.0012	3681 ± 5	99
4.2	osc,p		813	199	0.25	0.08	1.243 ± 0.040	0.3380 ± 0.0008	3654 ± 4	104
5.1	osc,p	3693 ± 5	522	208	0.40	0.06	1.333 ± 0.043	0.3468 ± 0.0011	3693 ± 5	98
6.1	osc,p		1002	402	0.40	0.08	1.396 ± 0.045	0.3222 ± 0.0008	3580 ± 4	97
7.1	osc,p	3677 ± 10	196	108	0.55	0.30	1.334 ± 0.044	0.3432 ± 0.0022	3677 ± 10	98
***G91/75 metachert, eastern end of the belt**										
1.1	osc,p		239	81	0.34	1.85	1.385 ± 0.028	0.3414 ± 0.0029	3669 ± 13	96
1.2	osc,p	o 3693 ± 7	295	82	0.28	0.00	1.273 ± 0.025	0.3469 ± 0.0017	3693 ± 7	101
2.1	osc,p		436	277	0.64	0.08	1.268 ± 0.024	0.3472 ± 0.0010	3695 ± 4	101
2.2	osc,p	o 3703 ± 4	562	367	0.65	0.11	1.280 ± 0.024	0.3491 ± 0.0010	3703 ± 4	101
2.3	osc,p		467	295	0.63	0.02	1.305 ± 0.024	0.3471 ± 0.0010	3694 ± 4	99
3.1	osc,p		92	62	0.68	2.21	1.357 ± 0.028	0.3407 ± 0.0036	3666 ± 16	97
4.1	osc,p	3678 ± 9	118	82	0.69	0.26	1.429 ± 0.028	0.3434 ± 0.0019	3678 ± 9	93
5.1	osc,p	3679 ± 8	142	119	0.84	0.40	1.324 ± 0.026	0.3437 ± 0.0019	3679 ± 8	99
6.1	osc,p	wm 3695 ± 6	233	289	1.24	0.98	1.406 ± 0.027	0.3469 ± 0.0019	3693 ± 8	94
6.2	osc,p		143	88	0.62	0.57	1.347 ± 0.028	0.3497 ± 0.0032	3706 ± 14	97
6.3	osc,p		114	74	0.65	0.27	1.281 ± 0.026	0.3466 ± 0.0023	3692 ± 10	101
G07/07 metachert/BIF in the felsic unit containing the Rosing (1999) 'early life' locality										
1.1	e,osc,p	wm 3689 ± 5	246	123	0.50	0.14	1.337 ± 0.054	0.3473 ± 0.0018	3695 ± 8	97
1.2	e,osc,p		168	77	0.46	0.04	1.194 ± 0.041	0.3452 ± 0.0018	3686 ± 8	106
1.3	e,osc,p		339	180	0.53	0.23	1.284 ± 0.054	0.3452 ± 0.0020	3686 ± 9	101
G07/08 metachert/BIF with island arc basalts, western part of the belt										
1.1	m,osc,eq	3698 ± 13	235	118	0.50	0.41	1.380 ± 0.057	0.3478 ± 0.0031	3698 ± 13	95
2.1	m,h,p,fr	3753 ± 10	561	377	0.67	0.06	1.404 ± 0.079	0.3608 ± 0.0024	3753 ± 10	92
3.1	m,osc,p	3679 ± 12	280	100	0.36	0.17	1.342 ± 0.042	0.3436 ± 0.0027	3679 ± 12	98
4.1	e,osc,p,fr	3690 ± 16	272	166	0.61	0.53	1.321 ± 0.074	0.3460 ± 0.0037	3690 ± 16	99
1.1.2. published data, reassessed										
G04/85 BIF, eastern part of the belt (Nutman et al., 2007)										
1.1	e,osc,eq	wm 3700 ± 12	114	67	0.59	0.21	1.268 ± 0.033	0.3480 ± 0.0034	3698 ± 15	101
1.2	e,osc,eq		108	53	0.49	0.15	1.303 ± 0.056	0.3487 ± 0.0040	3701 ± 18	99
2.1	e,osc,eq	wm 3699 ± 7	157	125	0.80	0.29	1.293 ± 0.025	0.3482 ± 0.0017	3699 ± 8	100
2.2	e,osc,eq		136	106	0.78	0.73	1.297 ± 0.039	0.3483 ± 0.0047	3699 ± 21	100
3.1	e,h/rex,eq		76	35	0.46	2.46	1.340 ± 0.041	0.3304 ± 0.0089	3619 ± 42	99
***IEh50ch/a metachert, eastern part of belt (Nutman et al., 2002)**										
1.1	osc,p	3671 ± 9	702	399	0.57	0.26	1.378 ± 0.043	0.3418 ± 0.0020	3671 ± 9	96
2.1	osc,p	3680 ± 12	187	101	0.54	0.44	1.350 ± 0.042	0.3438 ± 0.0026	3680 ± 12	97
3.1	osc,p	3699 ± 7	209	134	0.64	0.37	1.307 ± 0.041	0.3481 ± 0.0016	3699 ± 7	99
4.1	osc,p	3689 ± 16	166	99	0.60	0.39	1.330 ± 0.070	0.3460 ± 0.0035	3689 ± 16	98
5.1	osc,p	3693 ± 17	356	177	0.50	0.30	1.327 ± 0.038	0.3468 ± 0.0038	3693 ± 17	98
6.1	osc,p	wm 3693 ± 5	245	109	0.44	0.37	1.355 ± 0.040	0.3490 ± 0.0037	3703 ± 16	96
6.2	osc,p		340	186	0.55	0.27	1.274 ± 0.034	0.3466 ± 0.0011	3692 ± 5	101
7.1	osc,p	3693 ± 11	248	95	0.38	0.17	1.338 ± 0.046	0.3468 ± 0.0024	3693 ± 11	97
8.1	osc,p	3701 ± 15	192	99	0.52	0.21	1.271 ± 0.039	0.3487 ± 0.0034	3701 ± 15	101
9.1	osc,p	3694 ± 8	572	418	0.73	0.24	1.321 ± 0.035	0.3470 ± 0.0019	3694 ± 8	98
***G93/19 metachert with island arc basalts, western part of the belt (Nutman et al., 2002)**										
1.1	m,p,fr		879	354	0.40	0.89	1.562 0.130	0.3130 0.0027	3536 14	90
1.2	e,p,fr	o 3725 ± 3	620	326	0.53	0.17	1.335 0.030	0.3542 0.0006	3725 3	97
2.1	c,eq	wm 3706 ± 4	723	403	0.56	0.10	1.307 0.025	0.3474 0.0020	3696 9	99
2.2	c,eq		731	418	0.57	0.06	1.448 0.027	0.3493 0.0013	3704 5	91
2.3	r,eq		828	40	0.05	0.13	1.502 0.032	0.3157 0.0026	3549 13	93
2.4	c,eq		548	287	0.52	0.02	1.372 0.031	0.3500 0.0005	3707 2	95
2.5	r+c,eq		274	53	0.19	0.88	1.426 0.034	0.3332 0.0017	3632 8	94
3.1	m,p,fr		1019	780	0.76	0.13	1.386 0.021	0.3346 0.0017	3638 8	96
3.2	e,p,fr	o 3722 ± 3	365	145	0.40	0.10	1.374 0.032	0.3535 0.0008	3722 3	95
4.1	eq		621	6	0.01	0.66	1.624 0.059	0.3185 0.0010	3562 5	87
SM/GR/93/01 'metaconglomerate', eastern part of the belt (Kamber et al., 2005)										
01a	m,osc,p	wm 3740 ± 7	185	91	0.49	0.13	1.274 ± 0.034	0.3577 ± 0.0018	3740 ± 8	100

Table 1: SHRIMP U/Pb zircon analyses

Site	Grain/site type	Assessed/filtered 207Pb/206Pb grain age (Ma)	U ppm	Th ppm	Th/U	comm. 206Pb%	238U / 206/Pb ratio	207Pb / 206Pb ratio	207Pb/206Pb site date (Ma)	conc (%)
01b	e,osc,p		247	146	0.59	<0.01	1.132 ± 0.031	0.3573 ± 0.0035	3739 ± 15	109

1.2. felsic schists with volcanic or volcano-sedimentary protoliths

1.2.1. new data

G05/28+29 felsic schists, at the Rosing (1999) 'early life' locality

1.1	osc,eq		257	149	0.58	0.04	1.256 ± 0.050	0.3485 ± 0.0012	3701 ± 5	102
1.2	osc,eq	o 3723 ± 6	275	156	0.57	0.05	1.230 ± 0.040	0.3537 ± 0.0015	3723 ± 6	103
2.1	osc,p,fr		170	187	1.10	0.09	1.152 ± 0.041	0.3505 ± 0.0015	3709 ± 7	109
2.2	osc,p,fr	wm 3724 ± 6	153	139	0.91	0.01	1.373 ± 0.065	0.3559 ± 0.0025	3732 ± 11	95
2.3	osc,p,fr		239	284	1.19	0.05	1.358 ± 0.077	0.3529 ± 0.0017	3719 ± 8	96
2.4	osc,p,fr		119	106	0.88	0.09	1.211 ± 0.037	0.3508 ± 0.0024	3710 ± 11	105
3.1	m,osc,p	wm 3712 ± 2	825	1372	1.66	0.01	1.219 ± 0.045	0.3512 ± 0.0009	3712 ± 4	104
3.2	e,osc,p		701	974	1.39	0.01	1.211 ± 0.043	0.3526 ± 0.0013	3718 ± 5	104
3.3	e,osc,p		1120	2113	1.89	bld	1.194 ± 0.038	0.3507 ± 0.0009	3710 ± 4	106
3.4	e,osc,p		1041	1955	1.88	0.02	1.337 ± 0.050	0.3402 ± 0.0014	3664 ± 6	98

****G97/63 felsic schist, at the Harper and Jacobsen (1992) 142Nd anomally locality, eastern end of the belt**

1.1	osc,p	3704 ± 12	74	40	0.54	0.06	1.251 ± 0.033	0.3492 ± 0.0028	3704 ± 12	102
2.1	osc,p	3691 ± 5	122	97	0.79	0.09	1.289 ± 0.033	0.3463 ± 0.0012	3691 ± 5	100
3.1	osc,p	3702 ± 8	111	79	0.71	0.11	1.288 ± 0.031	0.3489 ± 0.0018	3702 ± 8	100
4.1	osc,p	3712 ± 25	116	58	0.50	0.12	1.292 ± 0.037	0.3511 ± 0.0058	3712 ± 25	100
5.1	osc,p	3705 ± 9	88	65	0.74	0.01	1.243 ± 0.034	0.3496 ± 0.0021	3705 ± 9	103
6.1	osc,p		178	149	0.84	0.08	1.532 ± 0.030	0.3501 ± 0.0016	3708 ± 7	87
7.1	osc,p		82	44	0.54	0.01	1.299 ± 0.159	0.3346 ± 0.0076	3638 ± 35	101
8.1	osc,p	3684 ± 11	71	53	0.75	0.02	1.305 ± 0.029	0.3449 ± 0.0025	3684 ± 11	100
9.1	osc,p	3708 ± 8	129	86	0.66	0.00	1.299 ± 0.028	0.3502 ± 0.0017	3708 ± 8	99
10.1	osc,p	3706 ± 7	68	38	0.56	0.17	1.269 ± 0.029	0.3498 ± 0.0016	3706 ± 7	101
11.1	osc,p	3694 ± 8	61	31	0.50	0.18	1.294 ± 0.035	0.3469 ± 0.0018	3694 ± 8	100
12.1	osc,p	3710 ± 9	99	67	0.68	0.03	1.342 ± 0.033	0.3506 ± 0.0021	3710 ± 9	97
13.1	osc,p	3698 ± 13	113	142	1.26	0.05	1.330 ± 0.040	0.3480 ± 0.0029	3698 ± 13	98
14.1	osc,p	3706 ± 8	137	80	0.58	0.02	1.331 ± 0.032	0.3497 ± 0.0019	3706 ± 8	98
15.1	osc,p	3717 ± 10	69	48	0.70	0.17	1.305 ± 0.038	0.3523 ± 0.0023	3717 ± 10	99
16.1	osc,p	3712 ± 8	158	81	0.51	0.03	1.320 ± 0.030	0.3511 ± 0.0018	3712 ± 8	98
17.1	osc,p	3709 ± 8	64	52	0.81	0.02	1.376 ± 0.046	0.3505 ± 0.0018	3709 ± 8	95

1.2.2. published data, reassessed

***G91/76 homogeneous felsic schist, eastern part of the belt (Nutman et al., 1996)**

1.1	osc,p	3713 ± 10	101	54	0.53	0.03	1.304 ± 0.028	0.3513 ± 0.0022	3713 ± 10	99
2.1	osc,p	3710 ± 8	133	82	0.61	0.43	1.287 ± 0.027	0.3508 ± 0.0019	3710 ± 8	100
3.1	osc,p		192	122	0.64	0.26	1.387 ± 0.028	0.3402 ± 0.0014	3663 ± 6	96
4.1	osc,p	3719 ± 6	182	82	0.45	0.11	1.339 ± 0.027	0.3527 ± 0.0013	3719 ± 6	97
5.1	osc,p	3717 ± 7	147	118	0.80	0.01	1.170 ± 0.024	0.3523 ± 0.0015	3717 ± 7	107
6.1	osc,p		154	47	0.31	0.64	1.483 ± 0.030	0.3368 ± 0.0017	3648 ± 8	91
7.1	osc,p	3711 ± 9	112	76	0.68	0.19	1.285 ± 0.027	0.3510 ± 0.0021	3711 ± 9	100
8.1	osc,p	3708 ± 5	203	156	0.77	0.00	1.301 ± 0.026	0.3502 ± 0.0012	3708 ± 5	99
9.1	osc,p		169	68	0.40	0.73	1.481 ± 0.030	0.3277 ± 0.0017	3606 ± 8	92
10.1	osc,p	3714 ± 5	266	135	0.51	0.01	1.327 ± 0.026	0.3516 ± 0.0012	3714 ± 5	98
11.1	osc,p	3699 ± 9	111	48	0.44	0.24	1.296 ± 0.027	0.3482 ± 0.0020	3699 ± 9	100
12.1	osc,p	3698 ± 6	227	183	0.81	0.05	1.330 ± 0.027	0.3480 ± 0.0014	3698 ± 6	98
13.1	osc,p	3700 ± 7	118	89	0.75	0.13	1.337 ± 0.028	0.3484 ± 0.0017	3700 ± 7	97
14.1	osc,p	3707 ± 5	205	159	0.78	0.02	1.330 ± 0.026	0.3501 ± 0.0012	3707 ± 5	98
15.1	osc,p	3702 ± 6	248	207	0.83	0.74	1.350 ± 0.027	0.3488 ± 0.0014	3702 ± 6	97
16.1	osc,p	3692 ± 6	170	93	0.55	0.21	1.294 ± 0.026	0.3466 ± 0.0013	3692 ± 6	100
17.1	osc,p	3694 ± 6	152	120	0.79	0.11	1.376 ± 0.028	0.3471 ± 0.0014	3694 ± 6	95
18.1	m,osc,p	3733 ± 12	54	34	0.62	0.30	1.359 ± 0.031	0.3560 ± 0.0028	3733 ± 12	95
18.2	e,osc,p		48	35	0.73	0.80	1.440 ± 0.037	0.3395 ± 0.0053	3660 ± 24	93
19.1	osc,p	3710 ± 5	255	121	0.47	0.08	1.301 ± 0.026	0.3506 ± 0.0012	3710 ± 5	99
20.1	osc,p	3705 ± 6	274	149	0.54	0.21	1.342 ± 0.027	0.3497 ± 0.0013	3705 ± 6	97
21.1	osc,p	3710 ± 9	98	63	0.64	0.20	1.289 ± 0.028	0.3506 ± 0.0022	3710 ± 9	100
22.1	osc,p	3710 ± 25	92	39	0.42	bld	1.314 ± 0.028	0.3506 ± 0.0057	3710 ± 25	98
23.1	osc,p	3697 ± 6	139	99	0.71	0.03	1.315 ± 0.027	0.3477 ± 0.0015	3697 ± 6	99

G93/75 clast-rich felsic schist, eastern part of the belt (Nutman et al., 1997)

1.1	p	3719 ± 8	114	96	0.84	bld	1.326 ± 0.027	0.3527 ± 0.0019	3719 ± 8	97
2.1	p	3723 ± 6	196	134	0.68	0.02	1.304 ± 0.026	0.3536 ± 0.0015	3723 ± 6	99
3.1	p	3723 ± 6	208	118	0.57	0.00	1.322 ± 0.026	0.3538 ± 0.0013	3723 ± 6	98
4.1	p	3690 ± 6	194	92	0.48	0.02	1.400 ± 0.028	0.3462 ± 0.0014	3690 ± 6	94
5.1	p	3717 ± 7	152	95	0.63	0.09	1.310 ± 0.026	0.3524 ± 0.0016	3717 ± 7	98
6.1	p	3705 ± 7	171	130	0.76	0.04	1.272 ± 0.026	0.3494 ± 0.0015	3705 ± 7	101
7.1	p	3711 ± 8	161	121	0.75	0.22	1.349 ± 0.027	0.3510 ± 0.0017	3711 ± 8	96
8.1	p	3692 ± 7	143	93	0.65	0.10	1.275 ± 0.026	0.3465 ± 0.0017	3692 ± 7	101
9.1	p	3691 ± 8	148	68	0.46	bld	1.318 ± 0.027	0.3463 ± 0.0018	3691 ± 8	99
10.1	p	3721 ± 10	84	43	0.52	0.02	1.350 ± 0.028	0.3532 ± 0.0022	3721 ± 10	96
11.1	p	3724 ± 6	196	150	0.77	0.01	1.348 ± 0.027	0.3540 ± 0.0014	3724 ± 6	96
12.1	p	3715 ± 8	147	117	0.80	0.09	1.335 ± 0.027	0.3518 ± 0.0018	3715 ± 8	97
13.1	p	3723 ± 7	192	152	0.79	0.06	1.356 ± 0.027	0.3537 ± 0.0015	3723 ± 7	96
14.1	p	3719 ± 8	115	50	0.43	bld	1.361 ± 0.028	0.3529 ± 0.0019	3719 ± 8	95
15.1	p	3713 ± 7	164	110	0.67	bld	1.340 ± 0.027	0.3514 ± 0.0015	3713 ± 7	97
16.1	p	3700 ± 7	195	90	0.46	0.19	1.361 ± 0.027	0.3485 ± 0.0015	3700 ± 7	96
17.1	p		214	58	0.27	0.11	1.437 ± 0.029	0.3258 ± 0.0014	3597 ± 7	95
18.1	p	3719 ± 11	77	52	0.67	0.37	1.324 ± 0.029	0.3529 ± 0.0026	3719 ± 11	97

Table 1: SHRIMP U/Pb zircon analyses

Site	Grain/site type	Assessed/filtered 207Pb/206Pb grain age (Ma)	U ppm	Th ppm	Th/U	comm. 206Pb%	238U / 206/Pb ratio	207Pb / 206Pb ratio	207Pb/206Pb site date (Ma)	conc (%)
19.1	p	3711 ± 6	231	186	0.81	0.24	1.340 ± 0.027	0.3508 ± 0.0014	3711 ± 6	97
20.1	p		181	125	0.69	0.22	1.313 ± 0.026	0.3432 ± 0.0016	3677 ± 7	99
21.1	p		44	31	0.69	0.14	1.297 ± 0.038	0.3394 ± 0.0037	3660 ± 17	101
22.1	p	3688 ± 8	150	60	0.40	bld	1.287 ± 0.034	0.3456 ± 0.0018	3688 ± 8	101
23.1	p	3712 ± 5	187	127	0.68	0.19	1.338 ± 0.035	0.3518 ± 0.0019	3715 ± 8	97
24.1	p	3710 ± 7	207	151	0.73	0.02	1.352 ± 0.035	0.3507 ± 0.0017	3710 ± 7	96
25.1	p	wm 3721 ± 5	187	136	0.73	0.09	1.296 ± 0.034	0.3526 ± 0.0017	3718 ± 7	99
25.2	p		161	109	0.68	bld	1.343 ± 0.035	0.3536 ± 0.0016	3723 ± 7	96
26.1	p	3751 ± 6	224	189	0.84	0.03	1.312 ± 0.034	0.3603 ± 0.0014	3751 ± 6	97
27.1	p	3727 ± 8	152	90	0.60	bld	1.280 ± 0.033	0.3545 ± 0.0018	3727 ± 8	100
28.1	p	3731 ± 10	103	67	0.65	0.11	1.306 ± 0.035	0.3556 ± 0.0023	3731 ± 10	98
29.1	t,p		296	148	0.50	0.10	1.394 ± 0.078	0.3277 ± 0.0012	3606 ± 6	97
30.1	t,p		155	99	0.64	0.17	1.464 ± 0.082	0.3304 ± 0.0027	3619 ± 13	93
31.1	t,p	3682 ± 25	114	106	0.93	0.42	1.340 ± 0.069	0.3442 ± 0.0055	3682 ± 25	98
32.1	c,p	3702 ± 5	658	651	0.99	0.09	1.264 ± 0.051	0.3488 ± 0.0011	3702 ± 5	102
32.2	r,p		604	54	0.09	0.03	1.379 ± 0.066	0.3065 ± 0.0023	3504 ± 12	100
G93/22, mylonitised felsic schist, western part of the belt (Nutman et al., 1997)										
1.1	p		61	62	1.01	9.94	2.087 ± 0.033	0.1566 ± 0.0065	2419 ± 72	104
1.2	p		421	494	1.17	1.44	2.612 ± 0.035	0.1627 ± 0.0011	2484 ± 11	84
2.1	p		1109	1029	0.93	0.05	2.848 ± 0.038	0.1420 ± 0.0004	2252 ± 5	86
2.3	p		952	855	0.90	0.17	2.745 ± 0.036	0.1538 ± 0.0004	2388 ± 5	84
3.1	p	wm 3710 ± 3	172	119	0.69	0.07	1.362 ± 0.019	0.3509 ± 0.0011	3711 ± 5	96
3.2	p		116	95	0.82	0.15	1.308 ± 0.019	0.3517 ± 0.0016	3715 ± 7	99
3.3	p		246	162	0.66	0.27	1.630 ± 0.022	0.3513 ± 0.0012	3712 ± 5	83
3.4	p		124	96	0.77	0.20	1.311 ± 0.019	0.3487 ± 0.0016	3701 ± 7	99
4.1	p		163	210	1.29	2.76	2.062 ± 0.029	0.1772 ± 0.0022	2627 ± 21	97
4.2	p		245	345	1.41	0.54	1.929 ± 0.027	0.1813 ± 0.0011	2665 ± 10	101
5.1	*contaminant*		*728*	*244*	*0.33*	*0.01*	*3.978 ± 0.052*	*0.093 ± 0.001*	*1497 ± 8*	*97*
1.3. garnet-mica schists with weathered mafic rock protoliths (all published data)										
SM/GR/97/31, eastern part of the belt (Kamber et al., 2005)										
03a		3707 ± 9	73	55	0.76	0.30	1.257 ± 0.034	0.3499 ± 0.0021	3707 ± 9	102
2a		3713 ± 6	204	114	0.56	0.13	1.261 ± 0.034	0.3513 ± 0.0014	3713 ± 6	101
SM/GR/97/22, eastern part of the belt (Kamber et al., 2005)										
2a		3702 ± 6	175	114	0.65	0.09	1.278 ± 0.035	0.3490 ± 0.0014	3702 ± 6	101
1a		3701 ± 16	66	39	0.59	0.41	1.237 ± 0.034	0.3486 ± 0.0037	3701 ± 16	103
SM/GR/93/57, eastern part of the belt										
06a		3718 ± 9	148	114	0.77	0.19	1.274 ± 0.034	0.3525 ± 0.0020	3718 ± 9	100
07a		3689 ± 7	131	89	0.68	0.13	1.317 ± 0.037	0.3459 ± 0.0017	3689 ± 7	99
08a		3691 ± 7	103	66	0.64	0.13	1.212 ± 0.033	0.3463 ± 0.0017	3691 ± 7	105
02-1a		3678 ± 13	132	58	0.44	1.08	1.337 ± 0.036	0.3434 ± 0.0030	3678 ± 13	98
04-1a		3715 ± 7	157	82	0.52	0.20	1.282 ± 0.036	0.3518 ± 0.0016	3715 ± 7	100
04-2a			179	120	0.67	0.26	1.452 ± 0.039	0.3473 ± 0.0016	3695 ± 7	91
03-1a	m,h,p,fr	wm 3707 ± 4	109	61	0.56	0.22	1.270 ± 0.036	0.3494 ± 0.0016	3704 ± 7	101
03-2a	e,osc,p		166	125	0.75	0.13	1.257 ± 0.034	0.3502 ± 0.0013	3708 ± 6	102
10a		3705 ± 4	605	430	0.71	0.07	1.247 ± 0.034	0.3495 ± 0.0008	3705 ± 4	102
2. Dividing sedimentary unit (all new data)										
G93/28 metacarbonate and chert rock, western part of the belt										
1.1	e,osc,p	3917 ± 10	170	81	0.48	0.20	1.142 ± 0.089	0.4022 ± 0.0028	3917 ± 10	104
2.1	e,osc,p		202	67	0.33	0.82	1.251 ± 0.095	0.3862 ± 0.0020	3856 ± 8	98
2.2	e,osc,p	o 3876 ± 15	103	46	0.45	0.69	1.199 ± 0.106	0.3912 ± 0.0040	3876 ± 15	101
3.1	m,osc,p	wm 3922 ± 7	192	87	0.45	0.09	1.149 ± 0.082	0.4050 ± 0.0026	3928 ± 10	103
3.2	m,osc,p		246	134	0.54	0.10	1.260 ± 0.112	0.4011 ± 0.0031	3913 ± 12	96
4.1	m,osc,p		282	247	0.88	0.23	1.187 ± 0.097	0.3601 ± 0.0019	3750 ± 8	105
4.2	m,osc,p	o 3765 ± 10	217	180	0.83	0.03	1.223 ± 0.082	0.3636 ± 0.0025	3765 ± 10	102
5.1	m,osc,p	3918 ± 7	204	144	0.70	0.13	1.187 ± 0.078	0.4025 ± 0.0019	3918 ± 7	101
6.1	m,osc,p	3810 ± 12	280	158	0.57	0.29	1.224 ± 0.070	0.3745 ± 0.0029	3810 ± 12	101
7.1	e,osc,p	o 3879 ± 16	280	146	0.52	0.21	1.158 ± 0.094	0.3920 ± 0.0042	3879 ± 16	104
7.2	e,osc,p		325	183	0.56	0.17	1.248 ± 0.071	0.3773 ± 0.0025	3821 ± 10	99
G07/22 BIF/chert, western end of the belt										
1.1	m,osc,p	3887 ± 20	306	154	0.50	0.07	1.187 ± 0.115	0.3943 ± 0.005	3887 ± 20	101
2.1	e,osc,p	3896 ± 19	153	85	0.55	0.67	1.293 ± 0.080	0.3965 ± 0.005	3896 ± 19	95
3.1	e,osc,p,fr	wm 3764 ± 6	195	151	0.77	1.01	1.212 ± 0.056	0.3597 ± 0.005	3749 ± 20	104
3.2	e,osc,p,fr		189	146	0.77	0.45	1.270 ± 0.086	0.3621 ± 0.003	3758 ± 14	100
3.3	e,osc,p,fr		160	130	0.81	0.22	1.236 ± 0.057	0.3641 ± 0.0015	3767 ± 6	102
4.1	m,osc,p,fr	o 3942 ± 51	91	44	0.48	1.81	1.305 ± 0.071	0.4090 ± 0.014	3942 ± 51	93
4.2	e,osc,p,fr		148	66	0.44	0.47	1.280 ± 0.069	0.3800 ± 0.0129	3832 ± 52	97
5.1	e,osc,p	3896 ± 10	358	288	0.80	0.22	1.180 ± 0.041	0.3967 ± 0.003	3896 ± 10	102
6.1	e,osc,p	3905 ± 19	347	266	0.77	1.55	1.288 ± 0.056	0.3990 ± 0.005	3905 ± 19	95
7.1	m,osc/h,p	3905 ± 52	229	111	0.48	0.40	1.245 ± 0.149	0.3991 ± 0.013	3906 ± 52	97
8.1	e,osc,p,fr	wm 3757 ± 6	384	267	0.70	0.53	1.287 ± 0.043	0.3634 ± 0.003	3764 ± 12	98
8.2	e,osc,p,fr		292	152	0.52	0.62	1.308 ± 0.100	0.3611 ± 0.0018	3754 ± 8	98
9.1	m,osc,p	3898 ± 22	124	44	0.35	1.74	1.227 ± 0.070	0.3972 ± 0.006	3899 ± 22	99
10.1	m,osc/h,p,fr	3918 ± 10	340	125	0.37	0.72	1.213 ± 0.049	0.4024 ± 0.003	3918 ± 10	99
G05/17 BIF, eastern part of the belt										
1.1	osc,eq	o 3770.8 ± 8	322	117	0.36	0.05	1.245 ± 0.056	0.3650 ± 0.0020	3771 ± 8	101

Table 1: SHRIMP U/Pb zircon analyses

Site	Grain/site type	Assessed/filtered 207Pb/206Pb grain age (Ma)	U ppm	Th ppm	Th/U	comm. 206Pb%	238U / 206/Pb ratio	207Pb / 206Pb ratio	207Pb/206Pb site date (Ma)	conc (%)
1.2	osc,eq		325	123	0.38	0.07	1.081 ± 0.072	0.3610 ± 0.0013	3754 ± 5	113
2.1	e,osc/rex,p	wm 3742 ± 7	409	208	0.51	0.17	1.239 ± 0.051	0.3573 ± 0.0022	3738 ± 9	102
2.2	e,osc/rex,p		413	365	0.88	0.22	1.299 ± 0.103	0.3594 ± 0.0028	3747 ± 12	98
G07/20 deformed granitic sheet, cutting dividing sedimentary unit										
1.1	e,osc,p,fr	3667 ± 15	429	184	0.43	1.31	1.328 ± 0.024	0.3410 ± 0.0034	3667 ± 15	99
2.1	m,osc,p,fr		116	60	0.52	7.06	1.450 ± 0.053	0.3196 ± 0.0219	3568 ± 110	95
2.2	e,osc,p,fr	3661 ± 4	933	606	0.65	0.32	1.396 ± 0.042	0.3397 ± 0.0010	3661 ± 4	95
3.1	e,osc,p,fr	3638 ± 11	266	189	0.71	0.10	1.329 ± 0.051	0.3346 ± 0.0024	3638 ± 11	99
4.1	e,osc,p,fr		426	260	0.61	0.85	1.480 ± 0.066	0.3041 ± 0.0094	3491 ± 49	95
5.1	m,osc,p		279	138	0.50	1.72	1.391 ± 0.070	0.3184 ± 0.0017	3562 ± 8	98
6.1	m,osc,p	3630 ± 28	439	371	0.85	0.54	1.420 ± 0.029	0.3327 ± 0.0060	3630 ± 28	95
7.1	comp,osc,p,fr	3659 ± 5	390	316	0.81	0.02	1.381 ± 0.056	0.3392 ± 0.0011	3659 ± 5	96
8.1	e,osc,p		1254	1137	0.91	0.11	1.401 ± 0.062	0.3280 ± 0.0019	3608 ± 9	96
9.1	e,osc,p		721	360	0.50	0.68	1.363 ± 0.042	0.3318 ± 0.0019	3625 ± 9	98
10.1	e,osc,p	3655 ± 8	169	110	0.65	0.04	1.305 ± 0.030	0.3382 ± 0.0017	3655 ± 8	100
11.1	e,osc,p		316	209	0.66	2.90	1.344 ± 0.039	0.3384 ± 0.0018	3655 ± 8	98
3. Southern ca. 3800 Ma terrane (all published data)										
****G93/25 fuchsite quartzite, marginal to 3806 Ma felsic volcanic unit (Nutman et al., 1997)**										
1.1	p	3872 ± 19	37	18	0.48	0.57	1.189 ± 0.059	0.3902 ± 0.0049	3872 ± 19	102
2.1	p	3856 ± 13	63	48	0.76	0.99	1.162 ± 0.041	0.3863 ± 0.0032	3856 ± 13	104
3.1	p	3865 ± 10	78	27	0.34	0.04	1.215 ± 0.049	0.3886 ± 0.0026	3865 ± 10	100
4.1	p	3851 ± 12	96	67	0.70	0.18	1.210 ± 0.039	0.3849 ± 0.0030	3851 ± 12	101
5.1	p	3849 ± 12	80	52	0.65	0.28	1.195 ± 0.038	0.3844 ± 0.0031	3849 ± 12	102
6.1	p	3848 ± 7	161	72	0.45	0.06	1.232 ± 0.036	0.3842 ± 0.0017	3848 ± 7	100
7.1	p	3832 ± 16	50	38	0.76	0.31	1.261 ± 0.050	0.3800 ± 0.0040	3832 ± 16	98
8.1	p	3846 ± 6	188	111	0.59	0.10	1.259 ± 0.038	0.3836 ± 0.0015	3846 ± 6	98
9.1	p	3857 ± 12	81	47	0.58	0.00	1.199 ± 0.047	0.3865 ± 0.0031	3857 ± 12	101
10.1	p	3857 ± 14	122	77	0.63	0.95	1.352 ± 0.030	0.3865 ± 0.0036	3857 ± 14	93
11.1	p	3842 ± 11	84	41	0.48	1.06	1.286 ± 0.042	0.3827 ± 0.0028	3842 ± 11	97
12.1	p	3876 ± 32	41	21	0.51	1.38	1.293 ± 0.063	0.3913 ± 0.0083	3876 ± 32	95
13.1	p	3853 ± 12	122	79	0.65	0.71	1.228 ± 0.026	0.3854 ± 0.0031	3853 ± 12	100
14.1	p	3846 ± 12	128	91	0.71	0.84	1.268 ± 0.025	0.3835 ± 0.0031	3846 ± 12	98
15.1	p	3820 ± 12	78	42	0.54	1.10	1.284 ± 0.038	0.3770 ± 0.0030	3820 ± 12	97
16.1	p	3843 ± 9	99	69	0.70	0.99	1.286 ± 0.034	0.3830 ± 0.0022	3843 ± 9	97
17.1	p	3897 ± 9	218	119	0.55	0.51	1.243 ± 0.020	0.3967 ± 0.0023	3897 ± 9	98
18.1	p	3852 ± 6	132	61	0.46	0.83	1.324 ± 0.037	0.3852 ± 0.0017	3852 ± 6	94
19.1	p	3836 ± 11	286	172	0.60	0.37	1.299 ± 0.049	0.3810 ± 0.0027	3836 ± 11	96
20.1	p	3857 ± 9	62	42	0.68	0.69	1.276 ± 0.029	0.3864 ± 0.0022	3857 ± 9	97
22.1	p	3847 ± 20	50	30	0.59	0.49	1.321 ± 0.049	0.3837 ± 0.0056	3847 ± 20	94
23.1	p	3865 ± 12	84	29	0.35	3.59	1.340 ± 0.037	0.3886 ± 0.0031	3865 ± 12	93
24.1	p	3862 ± 19	45	30	0.65	1.00	1.201 ± 0.112	0.3877 ± 0.0048	3862 ± 19	101
25.1	p	3858 ± 6	275	163	0.59	0.68	1.286 ± 0.037	0.3867 ± 0.0016	3858 ± 6	96
26.1	p	3837 ± 9	54	36	0.66	0.80	1.251 ± 0.039	0.3814 ± 0.0022	3837 ± 9	99
27.1	p	wm 3804 ± 4	228	106	0.46	0.30	1.335 ± 0.043	0.3747 ± 0.0030	3811 ± 12	95
27.2	p		364	212	0.58	1.08	1.329 ± 0.043	0.3730 ± 0.0010	3804 ± 4	95
28.1	p	3838 ± 12	123	81	0.66	1.33	1.334 ± 0.033	0.3815 ± 0.0030	3838 ± 12	94
29.1	p	3853 ± 8	238	172	0.72	1.83	1.296 ± 0.037	0.3854 ± 0.0020	3853 ± 8	96
30.1	p	3858 ± 6	116	49	0.42	0.29	1.254 ± 0.035	0.3866 ± 0.0015	3858 ± 6	98
31.1	p		124	81	0.66	19.91	1.270 ± 0.051	0.3898 ± 0.0064	3870 ± 25	97
32.2	p	wm 3850 ± 7	66	27	0.41	6.29	1.327 ± 0.086	0.3914 ± 0.0084	3876 ± 33	93
32.2	p		54	21	0.40	0.30	1.260 ± 0.034	0.3844 ± 0.0019	3849 ± 7	98
4. tectonic intercalations of younger (<3650 Ma) metasediments?										
4.1. New data										
G07/27 mylonitised chert/BIF, within northern ca. 3700 Ma terrane										
1.1	e,osc,p	wm 2557 ± 34?	890	146	0.16	0.02	2.239 ± 0.272	0.1760 ± 0.0078	2616 ± 76	91
1.2	e,osc,p		548	121	0.22	0.03	2.384 ± 0.125	0.1685 ± 0.0038	2542 ± 38	89
2.1	m,osc/rex,p,fr		1671	406	0.24	5.88	9.475 ± 0.220	0.1515 ± 0.0039	2363 ± 45	27
3.1	*contaminant*		*2317*	*1218*	*0.53*	*0.87*	*16.88 ± 0.894*	*0.059 ± 0.001*	*558 ± 37*	*67*
3.2	*contaminant*		*656*	*418*	*0.64*	*0.31*	*14.58 ± 0.704*	*0.056 ± 0.002*	*469 ± 71*	*91*
4.1	e,osc,p	wm 3697 ± 6	282	182	0.64	0.02	1.344 ± 0.032	0.3476 ± 0.0016	3697 ± 7	97
4.2	e,osc,p		159	84	0.53	0.10	1.266 ± 0.045	0.3480 ± 0.0026	3698 ± 12	102
5.1	osc/rex,p	3630 ± 8	291	171	0.59	0.09	1.486 ± 0.030	0.3327 ± 0.0016	3630 ± 8	91
6.1	e,osc,p	wm 3717 ± 6	182	84	0.46	0.04	1.289 ± 0.041	0.3521 ± 0.0016	3716 ± 7	100
6.2	e,osc,p		163	67	0.41	0.05	1.270 ± 0.066	0.3536 ± 0.0032	3722 ± 14	101
G07/02+04 siliceous unit, within southern ca. 3800 Ma terrane										
1.1	e,osc,p	3646 ± 22	58	39	0.68	0.26	1.401 ± 0.045	0.3363 ± 0.0049	3646 ± 22	95
2.1	m,h,p,fr	3653 ± 19	40	9	0.22	0.36	1.392 ± 0.064	0.3379 ± 0.0042	3653 ± 19	96
3.1	e,osc,p,fr	3898 ± 12	81	38	0.47	0.15	1.224 ± 0.037	0.3971 ± 0.0033	3898 ± 12	99
4.1	c,osc,p	2830 ± 14?	102	39	0.38	0.22	1.872 ± 0.081	0.2004 ± 0.0017	2830 ± 14	98
5.1	m,osc/rex,p,fr	3653 ± 9	153	41	0.27	0.19	1.488 ± 0.044	0.3378 ± 0.0019	3653 ± 9	91
6.1	m,h/rex,p	3670 ± 8	176	29	0.17	0.27	1.826 ± 0.091	0.3417 ± 0.0017	3670 ± 8	77
7.1	m,h,p,	3692 ± 50	293	10	0.03	0.08	1.313 ± 0.097	0.3465 ± 0.0112	3692 ± 50	99
8.1	m,osc,p	3717 ± 11	173	93	0.54	0.05	1.342 ± 0.060	0.3524 ± 0.0025	3717 ± 11	97
4.2. published data										
***MR81-318 fuchsite quartzite, within ca. 3800 Ma rocks (Nutman and Collerson, 1991)**										

Table 1: SHRIMP U/Pb zircon analyses

Site	Grain/site type	Assessed/filtered 207Pb/206Pb grain age (Ma)	U ppm	Th ppm	Th/U	comm. 206Pb%	238U / 206/Pb ratio	207Pb / 206Pb ratio	207Pb/206Pb site date (Ma)	conc (%)
1.1	p	3808 ± 8	47	30	0.63	0.11	1.225 ± 0.042	0.3742 ± 0.0020	3808 ± 8	101
2.1	c,p	3690 ± 3	447	266	0.59	0.44	1.226 ± 0.039	0.3461 ± 0.0007	3690 ± 3	104
2.2	r,p		354	1	<0.01	0.04	1.928 ± 0.062	0.1863 ± 0.0006	2710 ± 5	99
3.1	c,p	3841 ± 6	118	60	0.51	0.81	1.246 ± 0.041	0.3824 ± 0.0016	3841 ± 6	99
3.2	r,p		330	2	0.01	0.70	1.944 ± 0.063	0.1833 ± 0.0010	2683 ± 9	100
4.1	p	3791 ± 7	66	27	0.41	0.01	1.323 ± 0.044	0.3698 ± 0.0018	3791 ± 7	96
5.1	r,p		319	1	<0.01	0.13	1.983 ± 0.064	0.1835 ± 0.0007	2685 ± 6	98
6.1	p	3804 ± 4	228	111	0.49	0.02	1.246 ± 0.040	0.3732 ± 0.0009	3804 ± 4	100
7.1	p	3810 ± 7	71	38	0.54	0.09	1.250 ± 0.042	0.3747 ± 0.0018	3810 ± 7	99
8.1	p	3589 ± 10	128	85	0.67	1.47	1.441 ± 0.047	0.3241 ± 0.0021	3589 ± 10	95
9.1	p	3831 ± 6	97	44	0.46	0.08	1.214 ± 0.040	0.3798 ± 0.0014	3831 ± 6	101
10.1	p		56	24	0.43	0.35	1.518 ± 0.051	0.3598 ± 0.0023	3749 ± 10	87
11.1	p		642	470	0.73	0.14	1.293 ± 0.042	0.2880 ± 0.0004	3407 ± 2	108
12.1	p		118	45	0.38	0.47	1.516 ± 0.042	0.3395 ± 0.0016	3661 ± 7	89
12.2	p	o 3803 ± 6	183	88	0.48	0.44	1.325 ± 0.034	0.3729 ± 0.0015	3803 ± 6	95
13.1	p		397	152	0.38	0.30	1.256 ± 0.034	0.3489 ± 0.0009	3702 ± 4	102
13.2	p	o 3805 ± 5	221	82	0.37	0.03	1.262 ± 0.032	0.3734 ± 0.0012	3805 ± 5	99
14.1	r,p		260	2	0.01	0.17	2.071 ± 0.083	0.1847 ± 0.0007	2696 ± 7	94
15.1	p	3847 ± 3	198	169	0.86	0.03	1.255 ± 0.051	0.3839 ± 0.0008	3847 ± 3	98
16.1	p	3780 ± 4	140	122	0.87	0.15	1.253 ± 0.051	0.3672 ± 0.0010	3780 ± 4	100
17.1	p	3812 ± 5	149	66	0.44	0.07	1.262 ± 0.051	0.3751 ± 0.0012	3812 ± 5	99
19.1	p	wm 3653 ± 4	140	86	0.61	0.09	1.412 ± 0.057	0.3382 ± 0.0010	3655 ± 5	94
19.2	p		187	119	0.64	0.05	1.446 ± 0.037	0.3374 ± 0.0013	3651 ± 6	93
20.1	p		218	52	0.24	0.23	1.752 ± 0.070	0.2436 ± 0.0008	3144 ± 5	93
21.1	p	3730 ± 3	640	601	0.94	0.05	1.408 ± 0.035	0.3552 ± 0.0006	3730 ± 3	93
22.1	p	3798 ± 6	120	71	0.60	0.03	1.319 ± 0.034	0.3716 ± 0.0016	3798 ± 6	96
23.1	p	3635 ± 7	134	75	0.56	0.21	1.429 ± 0.037	0.3339 ± 0.0015	3635 ± 7	94
24.1	p	3816 ± 7	144	120	0.84	0.12	1.294 ± 0.034	0.3760 ± 0.0017	3816 ± 7	97
25.1	p	3628 ± 6	246	114	0.46	0.37	1.428 ± 0.037	0.3325 ± 0.0013	3628 ± 6	94
26.1	p	3866 ± 8	102	65	0.63	0.38	1.292 ± 0.034	0.3887 ± 0.0021	3866 ± 8	96
27.1	p	3811 ± 6	156	75	0.48	0.08	1.236 ± 0.032	0.3749 ± 0.0014	3811 ± 6	100
***288626 mylonitised siliceous rock, within ca. 3700 Ma northern terrane (Nutman et al., 1997)**										
1.1	p	wm 3709 ± 5	89	62	0.70	0.14	1.234 ± 0.020	0.3506 ± 0.0018	3710 ± 8	103
1.2	p		116	69	0.60	bld	1.258 ± 0.033	0.3503 ± 0.0018	3708 ± 8	102
2.1	p		69	38	0.55	0.21	1.349 ± 0.022	0.3497 ± 0.0016	3706 ± 7	96
2.2	p	o 3718 ± 6	170	131	0.77	0.04	1.313 ± 0.034	0.3526 ± 0.0014	3718 ± 6	98
3.1	p	3704 ± 5	144	61	0.42	bld	1.298 ± 0.021	0.3494 ± 0.0011	3704 ± 5	99
4.1	p	3436 ± 8	80	29	0.37	0.43	1.476 ± 0.024	0.2934 ± 0.0015	3436 ± 8	97
5.1	p	3490 ± 6	77	30	0.39	bld	1.283 ± 0.021	0.3038 ± 0.0012	3490 ± 6	106
6.1	p		136	55	0.41	0.24	1.222 ± 0.020	0.3269 ± 0.0012	3603 ± 6	107
6.2	p	o 3615 ± 7	131	65	0.50	0.27	1.329 ± 0.035	0.3296 ± 0.0015	3615 ± 7	100
7.1	p	3614 ± 8	46	23	0.51	bld	1.257 ± 0.022	0.3293 ± 0.0017	3614 ± 8	104
8.1	p	3677 ± 6	171	118	0.69	0.05	1.337 ± 0.035	0.3431 ± 0.0014	3677 ± 6	98
9.1	p	3693 ± 9	106	69	0.65	0.05	1.346 ± 0.036	0.3469 ± 0.0020	3693 ± 9	97
10.1	p	3551 ± 8	111	54	0.49	0.08	1.446 ± 0.038	0.3161 ± 0.0016	3551 ± 8	95
11.1	p	3587 ± 7	224	120	0.53	0.67	1.339 ± 0.034	0.3237 ± 0.0016	3587 ± 7	100
12.1	p	3551 ± 6	240	97	0.40	0.13	1.384 ± 0.035	0.3161 ± 0.0012	3551 ± 6	99

* by sample number indicates mid-early 1990s analysis without CL imaging
** by sample number indicates analysis guided by CL imaging, but images in deep storage in Australia
all uncertainties in the Table are given at 1 sigma.
Site: x.y, x=grain number, y=analysis number.
Grain and site character: p=prism, eq=small aspect ratio prism, fr=grain fragment, t=turbid
e=end analysis site, m=middle analysis site, r=rim, c=core
CL imagery: osc=oscillatory finescale zoning, h=homogeneous, hd=non-luminescent,
rex=recrystallised, comp=composite domains in analysis
Assessed/filtered ages: wm = weighted mean, o='oldest' age used
Common Pb correction: comm 206%= percentage of Pb that is non-radiogenic, based on measured 204Pb
and common Pb modelled as 3700 (northern terrane) 3800 Ma (southern terrane) of Cumming and Richards (1975)
bld = 204Pb not detected.

Table-2

Table 2

analysis	207Pb/206Pb age (Ma)	207Pb/206Pb	U	Th	Th/U	Hf	Ta	Sr	Y	La	Ce	Pr	Nd	Sm
G91/75 metachert														
a	3692	0.3466	274	84	0.31	12457	0.73	0.52	1267	0.77	25.7	0.48	3.13	3.19
b	3693	0.3469	215	265	1.23	10194	0.45	0.48	1258	0.69	38.4	0.96	9.73	9.61
c	3706	0.3498	199	170	0.86	11399	0.72	0.42	895	0.39	37.0	0.35	3.16	3.86
d	3697	0.3477	217	311	1.43	9995	0.51	0.59	2036	0.70	54.8	0.95	12.7	17.3
f	3691	0.3463	171	131	0.77	10414	0.63	0.37	1491	0.31	22.8	0.44	5.92	8.68
g	3701	0.3487	185	146	0.79	11447	0.70	0.44	938	0.27	29.4	0.22	2.64	3.91
IEh50 metachert														
b	3684	0.3448	584	543	0.93	9531	1.28	1.17	1859	2.61	33.1	2.20	14.4	12.9
c	3689	0.3458	215	125	0.58	10764	0.67	0.42	1199	0.16	13.9	0.18	2.90	5.15
d	3705	0.3496	288	212	0.74	8637	0.82	0.48	2145	0.61	23.4	0.35	4.22	6.56
e	3696	0.3476	548	557	1.02	9388	0.98	1.00	4244	21.4	150	13.9	88.3	73.0
f	3698	0.3480	232	145	0.63	9032	0.65	1.08	1399	3.79	27.9	2.24	14.5	10.7
h	3717	0.3522	207	88	0.42	10716	0.62	0.40	1168	2.40	15.1	1.09	7.05	7.07

Eu	Gd	Tb	Dy	Ho	Er	Tm	Yb	Lu
2.44	20.4	6.83	94.3	38.8	196	45.9	467	94.3
4.75	38.8	10.2	119	41.1	196	43.6	425	86.2
1.64	19.5	6.00	72.7	28.2	138	32.3	325	64.8
5.25	76.7	19.7	214	68.7	299	62.1	561	102
2.86	45.4	13.0	148	50.9	222	46.0	406	71.6
1.55	21.2	6.38	79.8	30.0	146	33.3	329	65.7
6.70	51.3	14.9	179	60.7	271	57.0	536	98.0
1.06	26.7	7.74	104	38.9	185	41.3	394	74.7
2.41	40.5	13.8	187	71.7	337	71.6	647	118
42.6	205.6	46.2	459	136	571	113	982	166
5.32	37.5	10.5	124	45.2	211	45.4	428	78.8
3.58	31.0	8.47	103	37.0	177	39.1	382	73.9

Figure-1

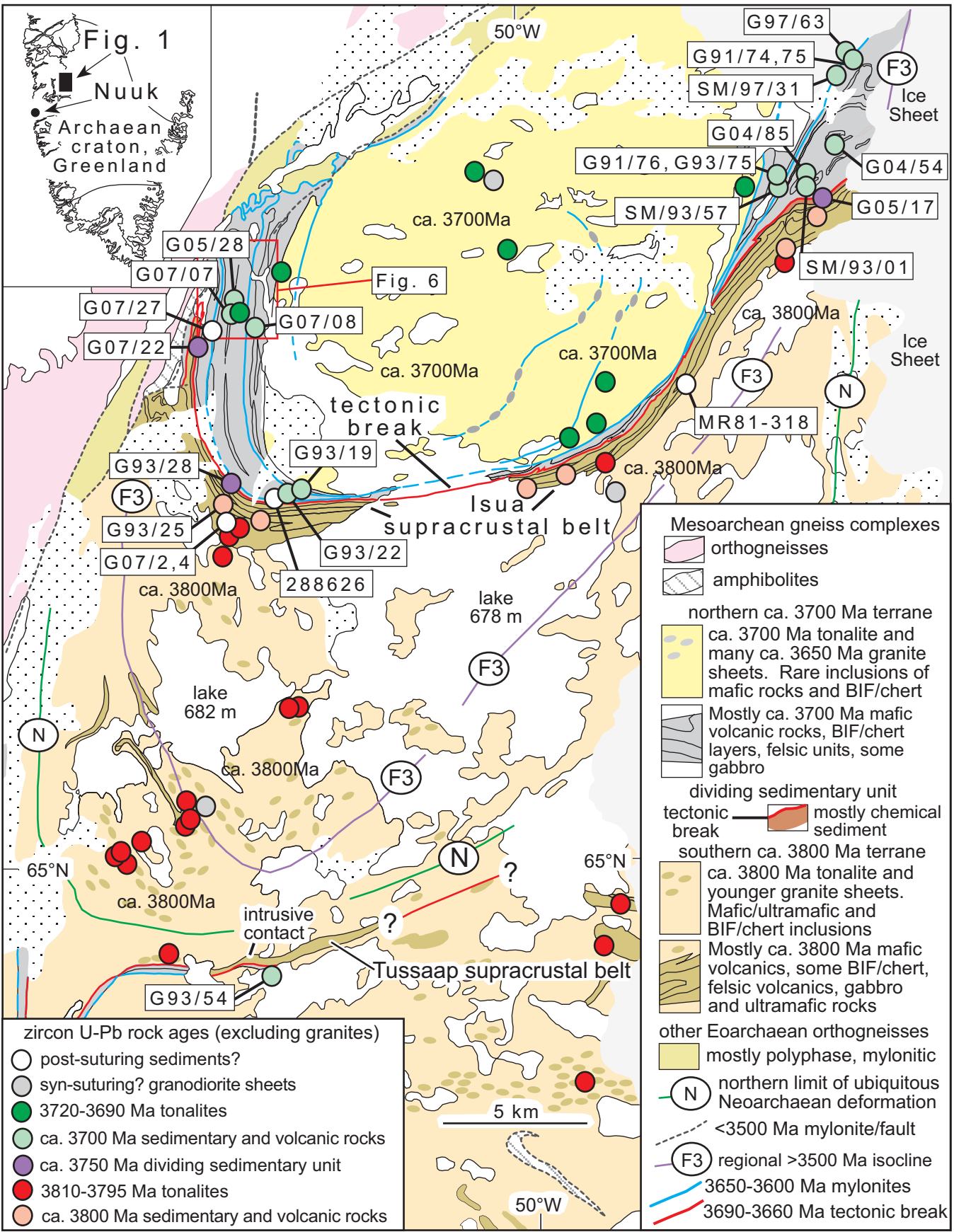
Fig. 1
Nuuk
Archaean craton, Greenland
50°W
G97/63
G91/74,75
SM/97/31
F3
Ice Sheet
G04/85
G04/54
G91/76, G93/75
G05/17
SM/93/57
SM/93/01
G05/28
G07/07
Fig. 6
G07/27
G07/08
G07/22
ca. 3700Ma
ca. 3800Ma
N
MR81-318
tectonic break
G93/19
G93/28
F3
G93/25
G07/2,4
G93/22
288626
Isua supracrustal belt
lake 678 m
lake 682 m
65°N
intrusive contact
Tussaap supracrustal belt
G93/54
5 km
zircon U-Pb rock ages (excluding granites)
post-suturing sediments?
syn-suturing? granodiorite sheets
3720-3690 Ma tonalites
ca. 3700 Ma sedimentary and volcanic rocks
ca. 3750 Ma dividing sedimentary unit
3810-3795 Ma tonalites
ca. 3800 Ma sedimentary and volcanic rocks
Mesoarchean gneiss complexes
orthogneisses
amphibolites
northern ca. 3700 Ma terrane
ca. 3700 Ma tonalite and many ca. 3650 Ma granite sheets. Rare inclusions of mafic rocks and BIF/chert
Mostly ca. 3700 Ma mafic volcanic rocks, BIF/chert layers, felsic units, some gabbro
dividing sedimentary unit
tectonic break
mostly chemical sediment
southern ca. 3800 Ma terrane
ca. 3800 Ma tonalite and younger granite sheets. Mafic/ultramafic and BIF/chert inclusions
Mostly ca. 3800 Ma mafic volcanics, some BIF/chert, felsic volcanics, gabbro and ultramafic rocks
other Eoarchaean orthogneisses
mostly polyphase, mylonitic
northern limit of ubiquitous Neoarchaean deformation
<3500 Ma mylonite/fault
regional >3500 Ma isocline
3650-3600 Ma mylonites
3690-3660 Ma tectonic break

Figure-2

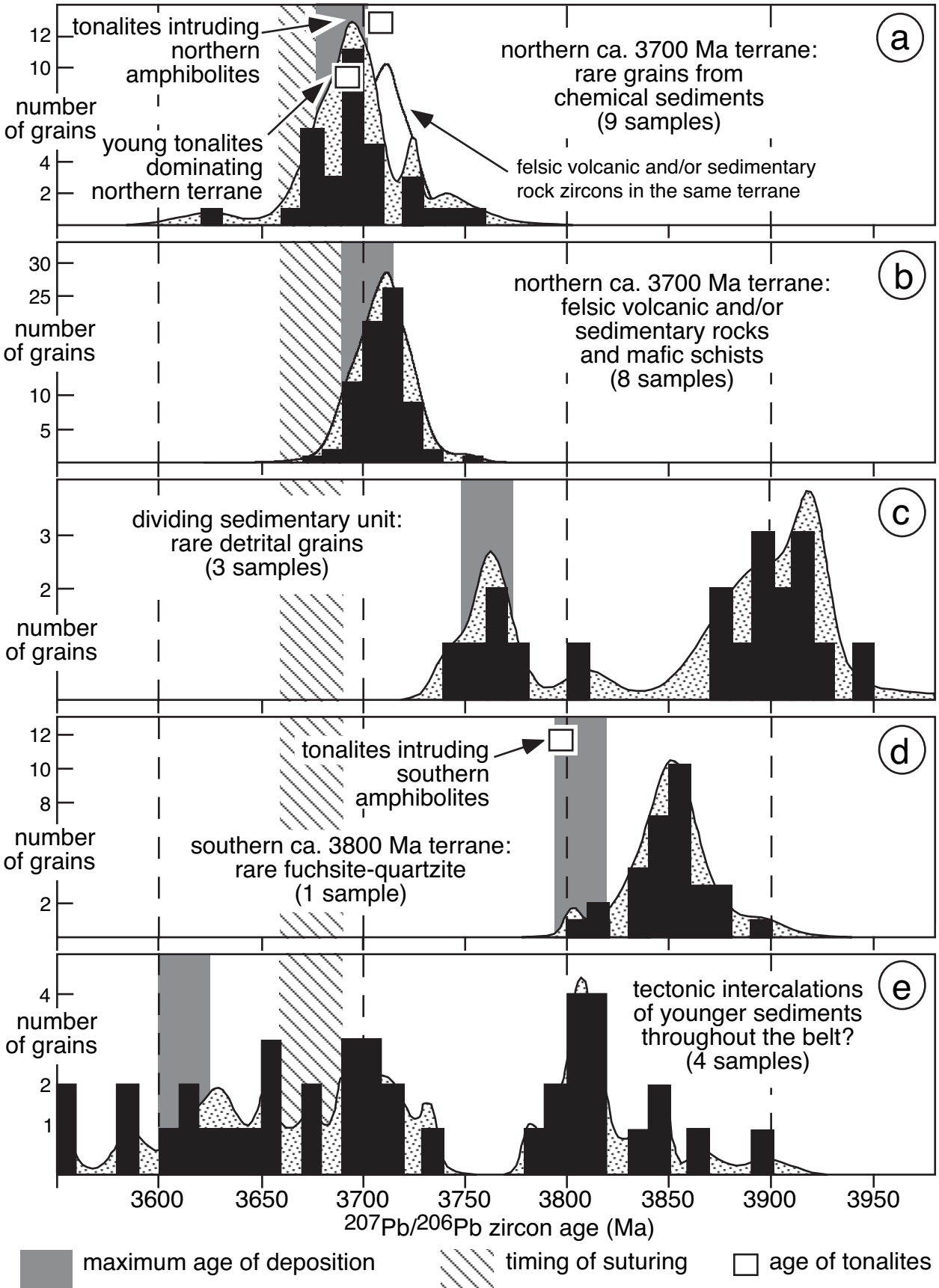
tonalites intruding northern amphibolites
young tonalites dominating northern terrane
northern ca. 3700 Ma terrane: rare grains from chemical sediments (9 samples)
felsic volcanic and/or sedimentary rock zircons in the same terrane
a
number of grains
northern ca. 3700 Ma terrane: felsic volcanic and/or sedimentary rocks and mafic schists (8 samples)
b
dividing sedimentary unit: rare detrital grains (3 samples)
c
tonalites intruding southern amphibolites
southern ca. 3800 Ma terrane: rare fuchsite-quartzite (1 sample)
d
tectonic intercalations of younger sediments throughout the belt? (4 samples)
e
3600
3650
3700
3750
3800
3850
3900
3950
207Pb/206Pb zircon age (Ma)
maximum age of deposition
timing of suturing
age of tonalites

Figure-3

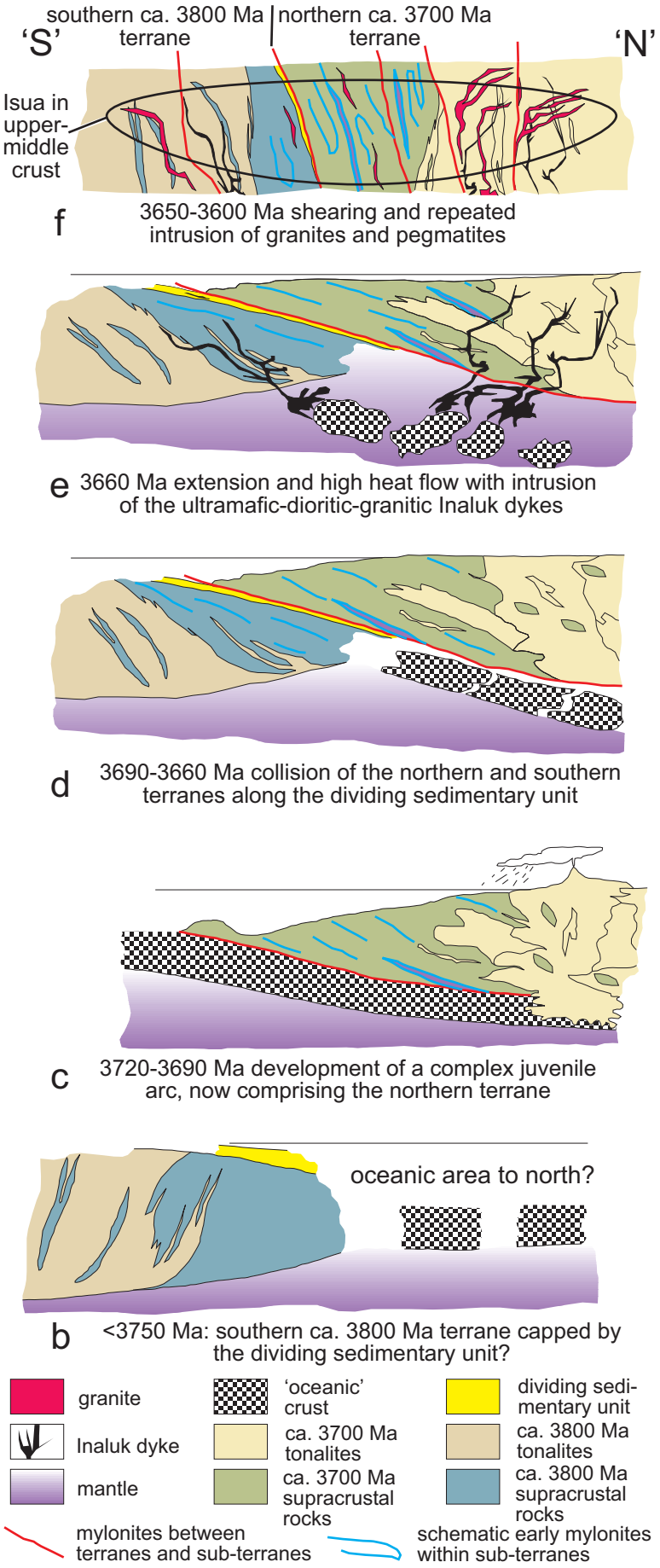
southern ca. 3800 Ma terrane
northern ca. 3700 Ma terrane
'S'
'N'
Isua in upper-middle crust
f
3650-3600 Ma shearing and repeated intrusion of granites and pegmatites
e
3660 Ma extension and high heat flow with intrusion of the ultramafic-dioritic-granitic Inaluk dykes
d
3690-3660 Ma collision of the northern and southern terranes along the dividing sedimentary unit
c
3720-3690 Ma development of a complex juvenile arc, now comprising the northern terrane
oceanic area to north?
b
<3750 Ma: southern ca. 3800 Ma terrane capped by the dividing sedimentary unit?
granite
Inaluk dyke
mantle
'oceanic' crust
ca. 3700 Ma tonalites
ca. 3700 Ma supracrustal rocks
dividing sedimentary unit
ca. 3800 Ma tonalites
ca. 3800 Ma supracrustal rocks
mylonites between terranes and sub-terranes
schematic early mylonites within sub-terranes

Figure-4

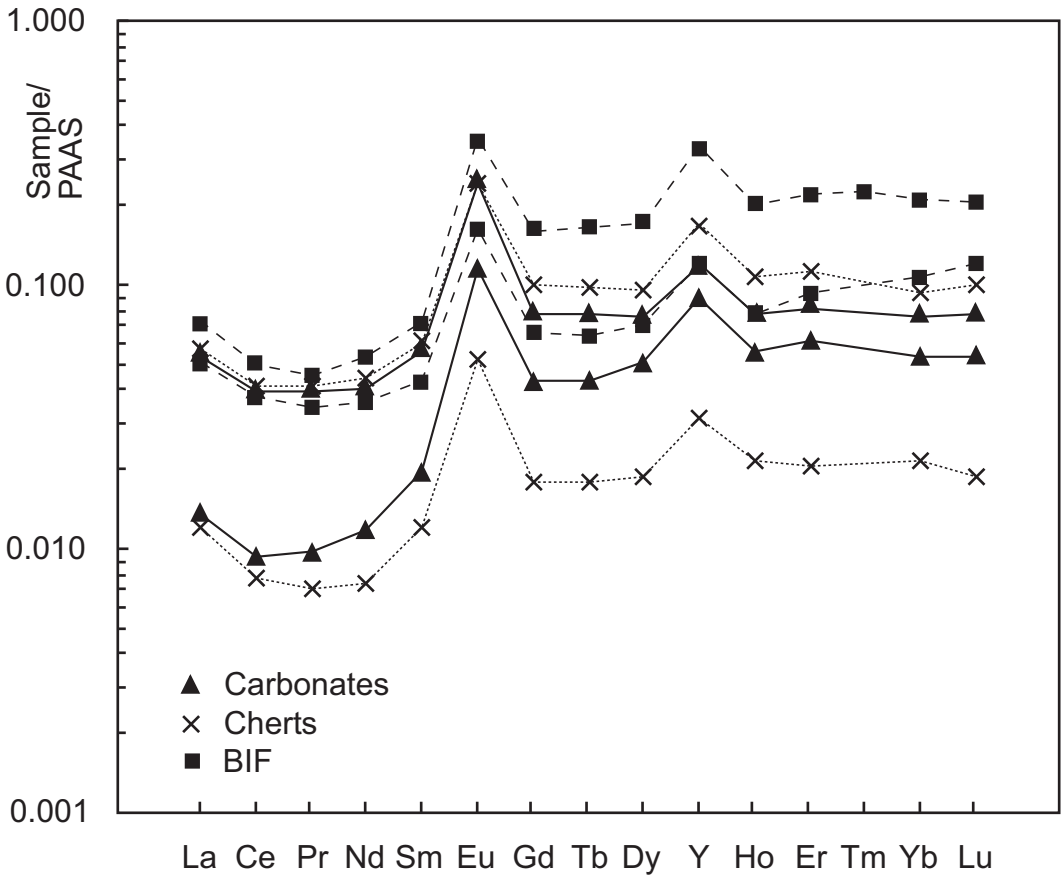
1.000
Sample/
PAAS
0.100
0.010
0.001
Carbonates
Cherts
BIF
La Ce Pr Nd Sm Eu Gd Tb Dy Y Ho Er Tm Yb Lu

Figure-5

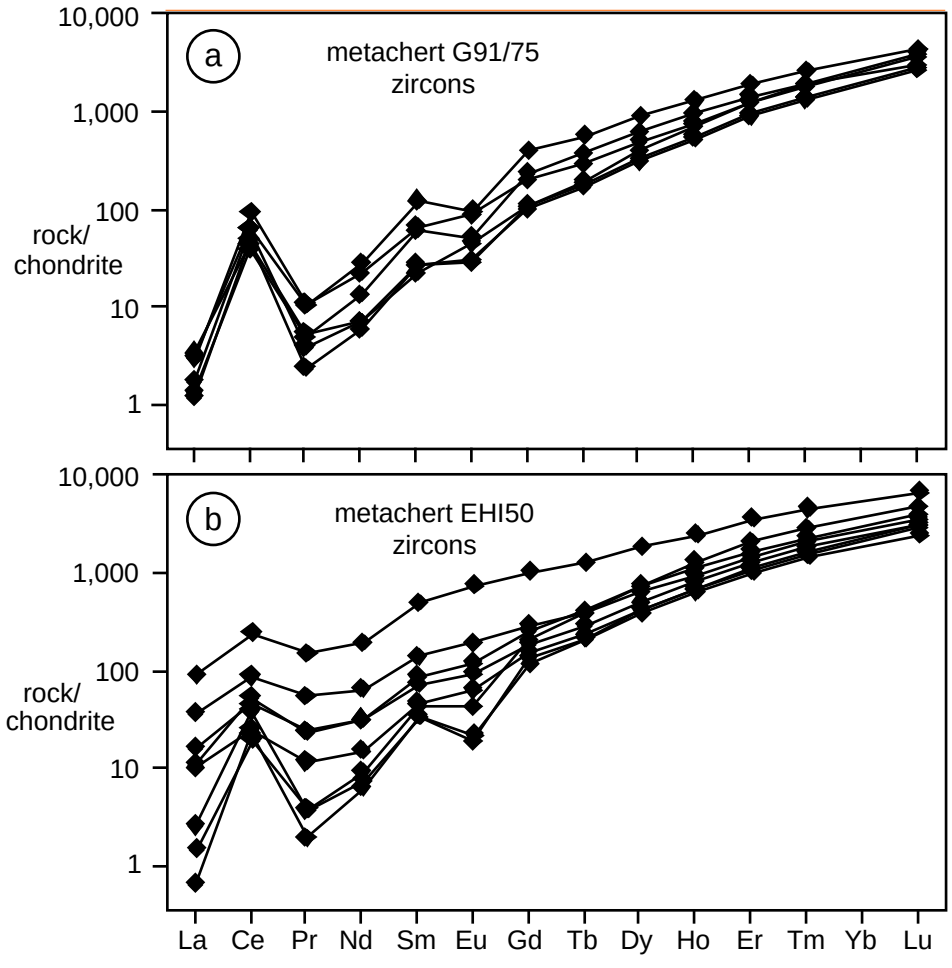
10,000
1,000
100
10
1
rock/
chondrite
a
metachert G91/75
zircons
10,000
1,000
100
10
1
rock/
chondrite
b
metachert EHI50
zircons
La
Ce
Pr
Nd
Sm
Eu
Gd
Tb
Dy
Ho
Er
Tm
Yb
Lu

Figure-6

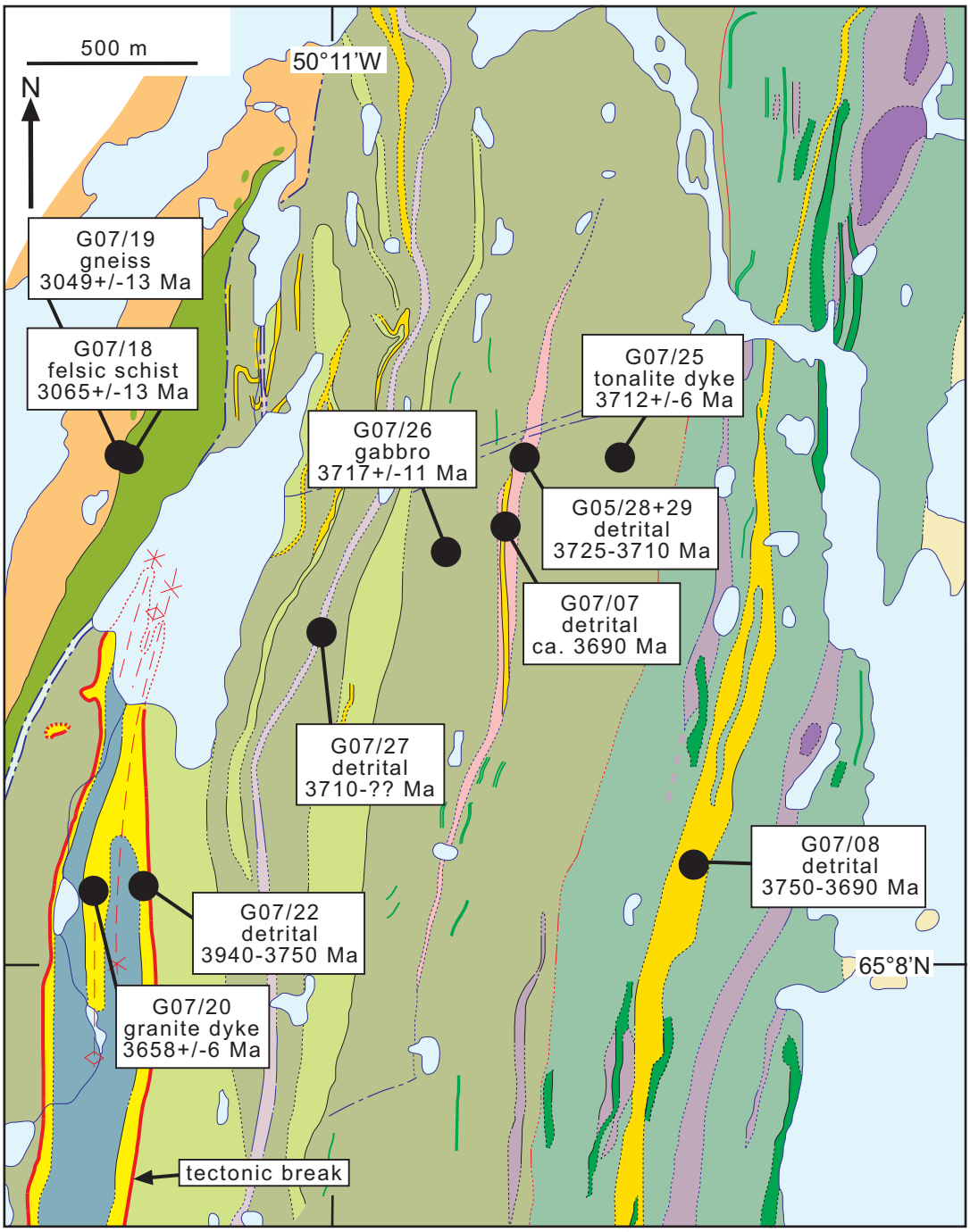

post-Mesoarchaean faults and mylonites

Mesoarchaean orthogneisses

Mesoarchaean amphibolites

Ameralik dykes 3510 Ma

mylonites associated with 3650-3600 Ma interleaving

3690-3660 Ma tectonic break between northern and southern terranes

Dividing sedimentary unit deposited between 3750-3690 Ma

cherts, siliceous carbonates and BIF, with minor detritus including 3940-3750 Ma zircons

Southern terrane ca. 3800 Ma

>3800 Ma amphibolites of mostly island-arc tholeiite affinity

Northern terrane 3720-3690 Ma

imbricate faults internal to the northern terrane

BIF and cherts with mostly 3700-3690 Ma zircons

3720-3710 Ma tonalites

3710-3700 Ma felsic volcanic and sedimentary rocks

ca. 3710-3700 Ma mafic and intermediate volcanic rocks

ca. 3715 Ma amphibolites of mostly island-arc tholeiite and picrite affinity

>3715 Ma amphibolites of boninitic chemical affinity

>3715 Ma schistose ultramafic rocks

>3715 Ma relict mantle dunitic rocks

Figure-7

Click here to download high resolution image

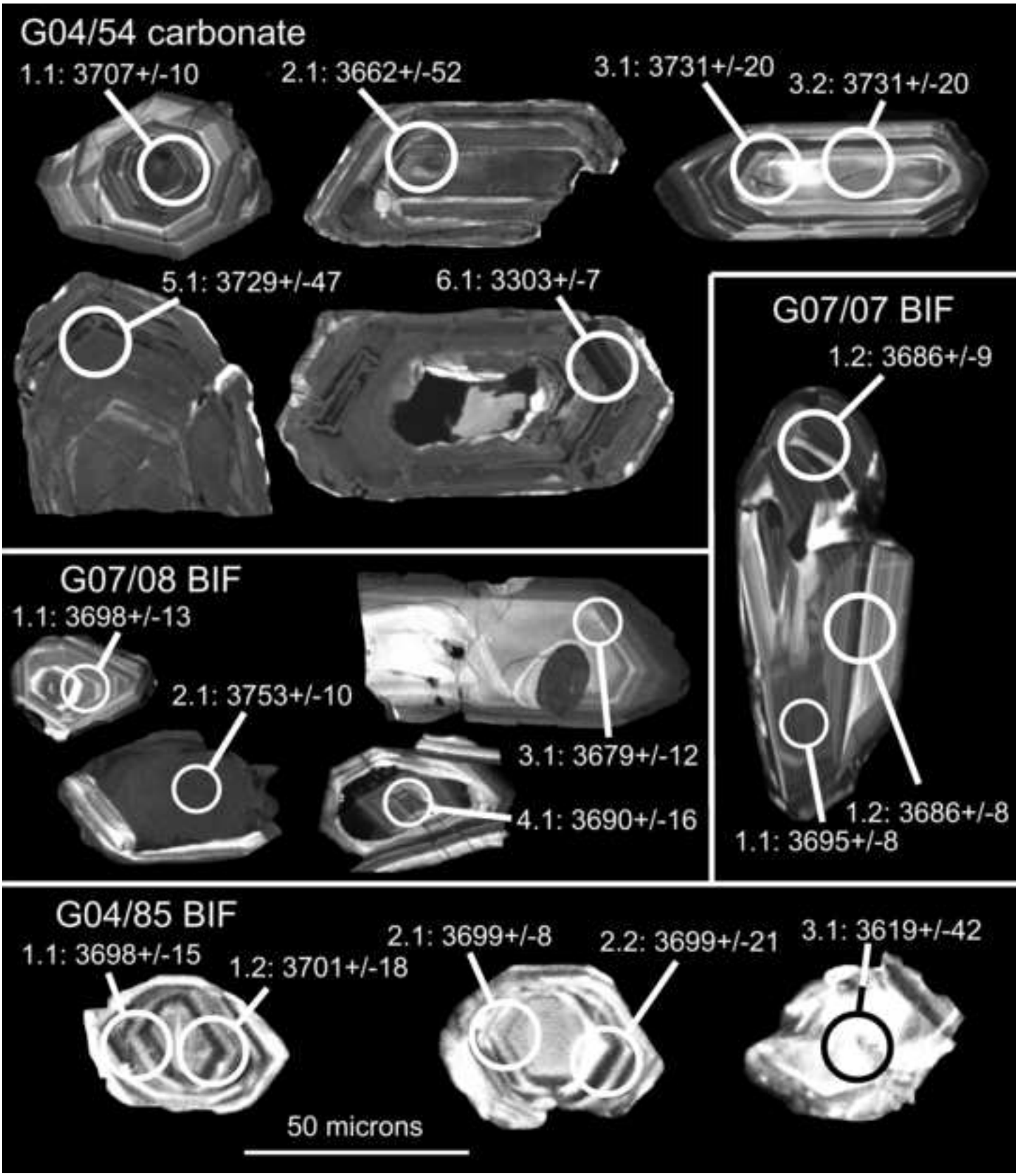

Figure-8

Click here to download high resolution image

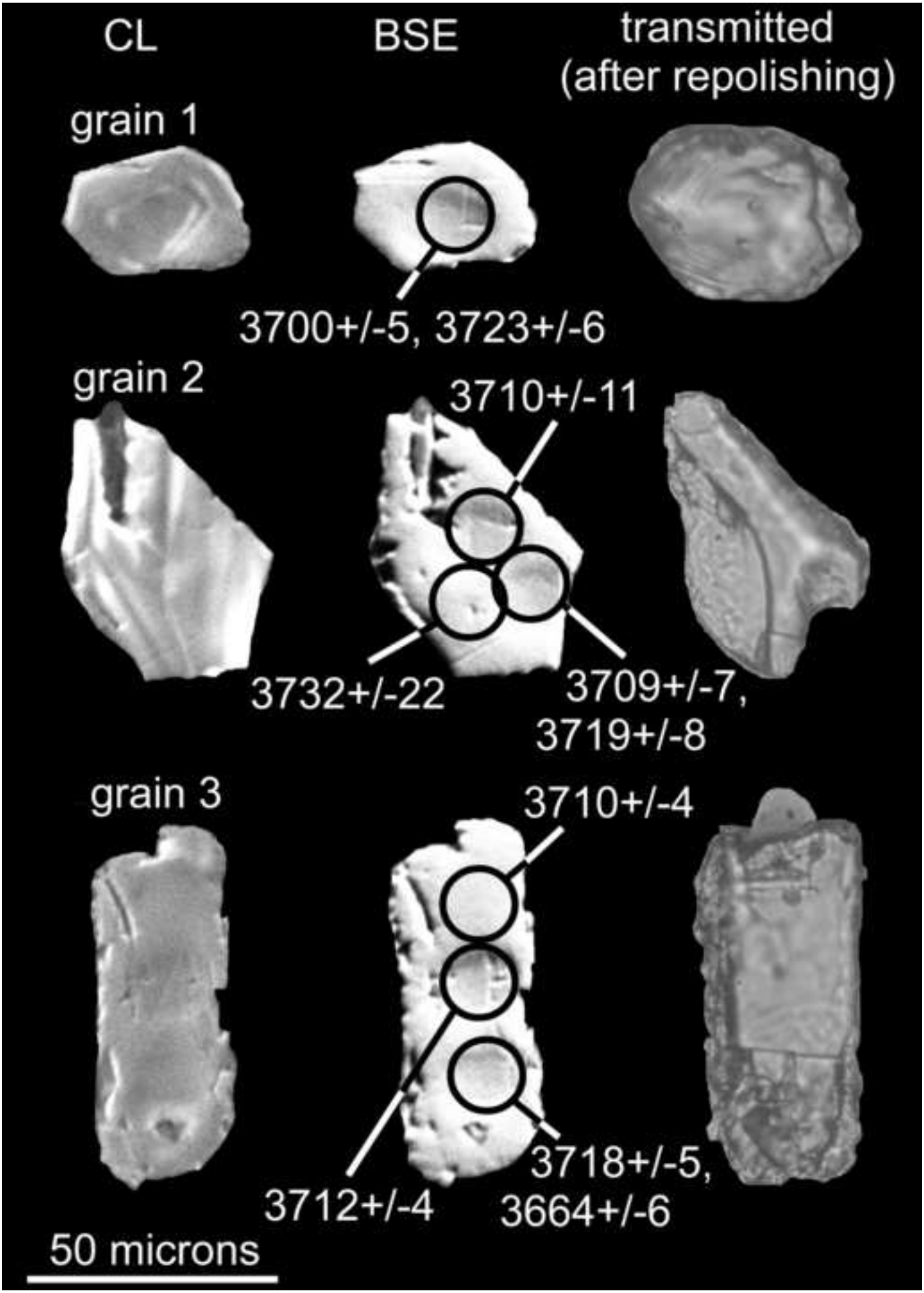

Figure-9

Click here to download high resolution image

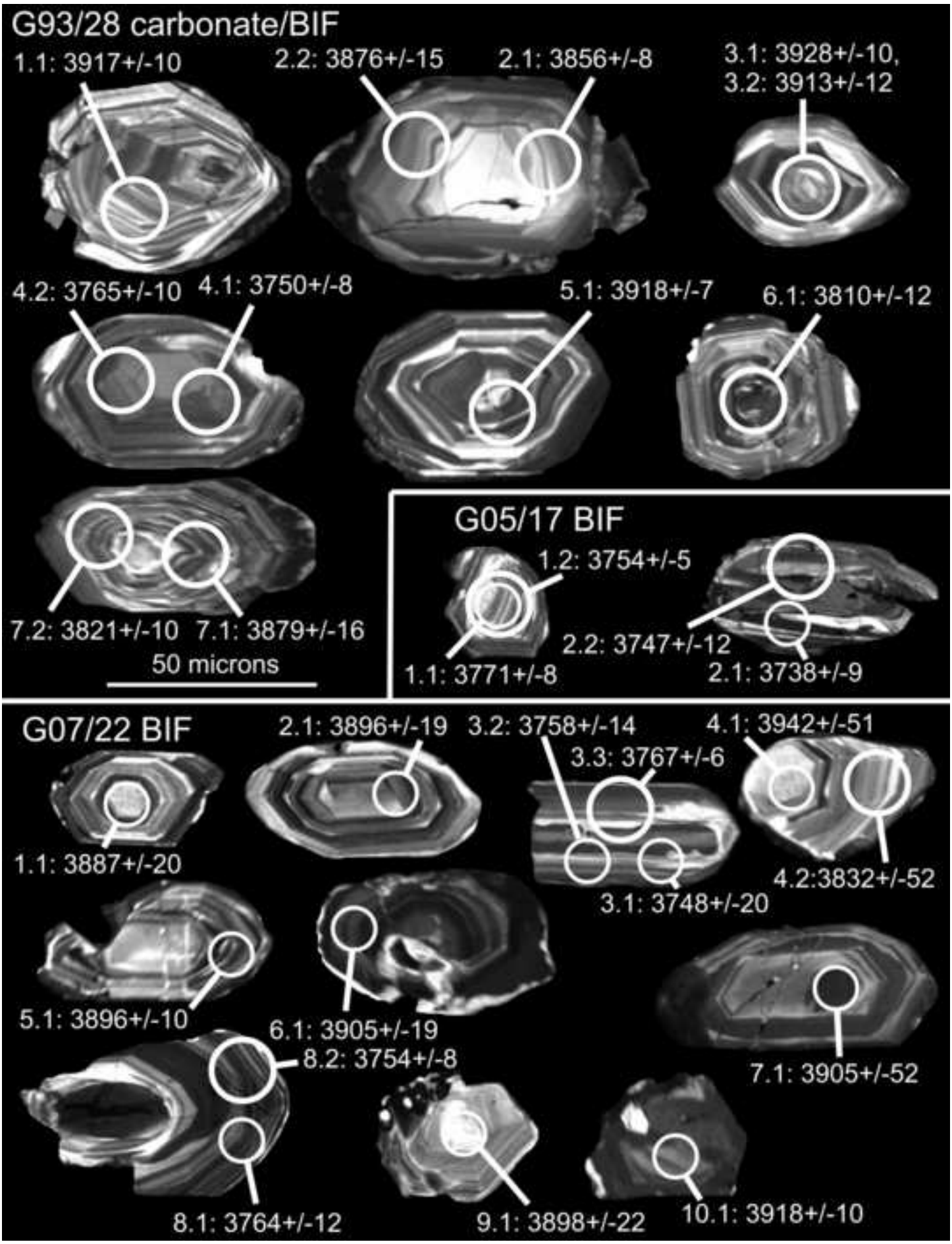

Figure-10
Click here to download high resolution image